No 547

January 2025

CefES

Center for European Studies

PAPER SERIES

Extreme Weather in Europe: Determinants and Economic Impact

Marcelle Chauvet, Claudio Morana, Murilo Silva

The Center for European Studies (CefES-DEMS) gathers scholars from different fields in Economics and Political Sciences with the objective of contributing to the empirical and theoretical debate on Europe.

DIPARTIMENTO DI ECONOMIA, METODI QUANTITATIVI E STRATEGIA DI IMPRESA

UNIVERSITÀ DEGLI STUDI DI MILANO BICOCCA

Extreme Weather in Europe: Determinants and Economic Impact

Marcelle Chauvet[+], Claudio Morana[*,*], Murilo Silva[§]

[+,§]University of California Riverside

[*]University of Milano-Bicocca

[*]Center for European Studies (CefES)

[*,+]Rimini Centre for Economic Analysis (RCEA-Europe ETS; RCEA-HQ)

[*]Center for Research on Pensions and Welfare Policies (CeRP)

December 2024

Abstract

This paper investigates the linkage between deteriorating extreme weather conditions and anthropogenic GHG emissions and their economic impact on 40 European countries. The analysis employs the European Extreme Events Climate Index (E3CI) and its seven subcomponents, i.e., extreme maximum and minimum temperatures, wind speed, precipitation, droughts, wildfires, and hail. Using an innovative panel regression-based trend-cycle decomposition approach, we find support for the contribution of human-made GHG emissions to the deterioration of underlying extreme weather conditions and their highly nonlinear pattern. We then conduct a Growth-at-Risk analysis within a quantile panel regression framework to assess the economic implications of our findings. We show that deteriorating extreme weather conditions, as measured by the E3CI index, negatively impact the entire GDP growth rate distribution. Yet the impact on the downside risk to growth is much more substantial than the upside risk. This result holds for various E3CI components, such as rising extreme maximum temperature, wind speed, drought, and wildfires.

Keywords: climate change, extreme weather events, global warming, GHG emissions, trend-cycle decomposition, Growth-at-Risk, panel quantile regressions, Europe

JEL classification: C21, C23, Q51, Q54

[*]Address for correspondence: Claudio Morana, Università di Milano - Bicocca, Dipartimento di Economia, Metodi Quantitativi e Strategie di Impresa, Piazza dell'Ateneo Nuovo 1, 20126, Milano, Italy. E-mail: claudio.morana@unimib.it.

1 Introduction

Greenhouse gas (GHG) concentrations have increased since the Industrial Revolution due to human activities, ultimately causing the Earth's surface temperature to rise, the so-called Global Warming effect. As Earth's climate has warmed, more frequent and intense weather events have been observed worldwide. A warming climate can contribute to the intensity of heat waves by increasing the chances of very hot days and nights. Climate warming also increases evaporation on land, which can worsen drought and create conditions more prone to wildfires and a more extended wildfire season. A warming atmosphere is also associated with heavier precipitation events (rain and snowstorms) through increases in the air's capacity to hold moisture. Earth's warmer and moister atmosphere and warmer oceans make it likely that the strongest hurricanes will be more intense, produce more rainfall, affect new areas, and possibly be more extensive and longer-lived. These consequences are expected to become more extreme in a warming climate, potentially leading to sizable economic and human losses (National Academies of Sciences, 2020).

There is a growing empirical literature on the economic impact of climate change (see the surveys by Auffhammer, 2018; Moore et al., 2024). A simple neoclassical growth model predicts that disasters destroying part of the capital stock lead to lower actual output in the short term. These effects would dissipate over time as reconstruction takes place. Noy (2009) and Kiley (2024) find that developing countries and smaller economies might face more significant output declines than developed countries or larger economies following a disaster of similar relative magnitude. This finding aligns with the higher adaptation ability likely possessed by developed countries. Felbermayr and Groschl (2014) show that geophysical disasters affect developing countries more strongly, while meteorological events developed countries. This finding might reflect their different geographical location, i.e., primarily the Northern Hemisphere for developed countries and mainly the Southern Hemisphere for developing countries, and how evolving weather conditions manifest across geographical zones. Other studies have identified some climatic events that had more persistent consequences for activity. For instance, Kahn et al. (2021) find that per-capita real output growth across countries is adversely affected by persistent changes in temperature above or below its historical norm. Kotz et al. (2021) find that daily fluctuations of temperatures can affect output, especially in low-latitude, low-income regions, while Kotz et al. (2022) show that economic growth rates are reduced by increases in the number of wet days and in extreme daily rainfall, with high-income nations being the most strongly hindered. The most recent evidence available for European countries, such as Usman et al. (2024), points to an aggregate demand channel through which raising economic uncertainty, income losses, disruptions, and emigration arising from climatic events might persistently depress economic activity and employment and endogenously lower long-term output. They find that the impact of extreme weather events in Europe is heterogeneous across event types (droughts, heatwaves, and floods) and regional relative income characteristics and intensifies over time. This latter characterization also aligns with the findings of Natoli (2023) for the US and Ciccarelli and Marotta (2024) for OECD countries that disasters can lower output by reducing aggregated demand.

In light of the ongoing GHG emissions trend and available empirical evidence, this paper addresses the concern for the economic impact of deteriorating extreme weather conditions in Europe. Europe is a region worth studying because it is warming faster

than the global average. The mean annual temperature over European land areas in the last decade was 2.12 to 2.19^{o}C warmer than during the pre-industrial period. Since instrumental records began, the warmest year in Europe is 2020, and the second warmest is 2023. In addition, projections show that temperatures across European land areas will continue to increase throughout this century at a rate higher than the global average.

The work most closely related to our paper is Kiley (2024), who first set the assessment of the economic costs of climate change in the Growth-at-Risk framework of Adrian et al. (2019), implementing it in a panel quantile framework. This methodology yields insights into per capita GDP growth distribution rather than its mean component only. Thus, it is ideal to tackle climate change's worrying tail risks. However, our study differs from Kiley (2024) in many respects. Using an innovative econometric procedure allowing for a trend-cycle decomposition within a panel regression framework, we first examine how anthropogenic GHG emissions drive underlying extreme weather conditions, as measured by the European Extreme Events Climate Index (E3CI) and its seven subcomponents, available for 40 European countries since 1981. Our analysis focuses on extreme maximum and minimum temperatures, wind speed, precipitation, droughts, wildfires, and hail. To the authors' knowledge, no previous study has been based on such a detailed dataset. The approach builds on Morana (2024) and Morana and Sbrana (2019). It directly exploits variation in extreme weather events across European countries over time, conditioning the extraction of the trend component on their likely determinant, i.e., radiative forcing, measured by changes in the atmospheric global abundance of long-lived, well-mixed greenhouse gases. We also indirectly control for the contribution of natural phenomena that impact weather behavior at low frequencies, such as the Atlantic Multidecadal Oscillator or AMO. The approach allows us to account for cross-county commonalities and heterogeneity. In this respect, we build on the idea that climate change is a global externality, i.e., one country's emissions affect all countries by adding to the stock of heat-warming gases in the Earth's atmosphere, from which extreme events increase in severity and frequency. We find that the common component is strongly dominant over idiosyncratic components, consistent with the global nature of climate change and the additional contribution of natural oscillators with long periodicity and global impact. This result aligns with the recent findings of Bilal and Kanzig (2024), who also highlight the importance of considering common effects when studying climate change. Overall, our study yields further evidence of the contribution of human-made GHG emissions to the deterioration of underlying extreme weather conditions and their highly nonlinear pattern.

We then exploit the above results in the Growth-at-Risk analysis, where we consider the multifaceted dimensions of deteriorating weather conditions by assessing the impact of various potential sources of economic, financial, and human losses beyond rising average temperatures. In this respect, we use the estimated underlying components for the E3CI index and its seven subcomponents to assess the potential effects of extreme temperatures (maximum and minimum), droughts, extreme precipitation, wildfires, extreme wind speed, and hail, in addition to overall weather conditions, on economic growth in Europe. As we focus on the current trend of the various extreme weather indicators, our assessment of their economic impact is consistent with a "business-as-usual" GHG growth scenario. We expect our broader conditioning set to lead to an accurate assessment of the economic impact of rising physical risk in Europe. We find that the linkage between deteriorating weather conditions, measured by the E3CI index, and the distribution of economic growth are clear-cut and show the downside risks to growth being

much more affected than the central tendency or upside risks. The negative impact of deteriorating weather conditions on the lowest quantiles of GDP growth is about fourfold that of the highest quantiles. Using single E3CI component regressions, we also find the downside risk to growth stronger than the upside risk for the extreme maximum temperature, wind speed, drought, and wildfire indicators. On the other hand, for the extreme minimum temperature and precipitation indicators, the upside risk to growth is more affected than the central tendency or the downside risks to growth. We obtained similar findings when we jointly assessed the impact of the E3CI subcomponents, also finding a negative economic impact for hail. Under a business-as-usual scenario, extreme weather episodes might generate a median contraction in trend real per capita GDP growth of about -0.15% per year.

The rest of the paper is as follows. Section 2 presents the framework for modeling evolving climatic conditions. Section 3 describes the data used in this study. Section 4 analyzes the extreme weather series trend developments. Section 5 discusses the framework for assessing growth-at-risk from climate change, including key aspects of the quantile regression approach and empirical results. Section 6 concludes.

2 Modeling evolving underlying extreme weather

Consider the vector of N country observations for the generic extreme weather indicator, as, for instance, extreme maximum temperature, at period t $\{\mathbf{y}_t\}$. The multivariate decomposition into medium to long-term (MLT) and short-term (ST) components can be written as

$$\mathbf{y}_t = \mathbf{m}_t + \mathbf{s}_t, \tag{1}$$

where $\mathbf{m}_t$ is the $(N \times 1)$ vector of MLT components, and $\mathbf{s}_t$ is the $(N \times 1)$ zero-mean vector of ST components. The vectors $\mathbf{m}_t$ and $\mathbf{s}_t$ are assumed to be orthogonal. As detailed below, the decomposition is implemented using a panel data regression approach within an Autometrics general-to-specific procedure (Hendry et al., 2008).

2.1 The generic country *MLT-ST* decomposition

Consider the generic n, t element in the vector $\mathbf{y}$, i.e., $y_{n,t}$, $n = 1, .., N$, $t = 1, .., T$, yielding the tth period observation for the extreme weather indicator $\mathbf{y}$ for the generic nth country. The generic decomposition equation is then

$$y_{n,t} = m_{n,t} + s_{n,t}, \tag{2}$$

where $\{m_{n,t}\}$ and $\{s_{n,t}\}$ are the generic MLT and ST components, respectively. It is assumed that $\{s_{n,t}\}$ is zero-mean and orthogonal to $\{m_{n,t}\}$. Following Morana (2024), $m_{n,t}$ is the real valued function

$$\begin{aligned} m_{n,t} &= \theta_{0,n} + \sum_{j=1}^{j^*} \theta_{s,n,j} \sin(2\pi j \frac{t}{T}) + \sum_{j=1}^{j^*} \theta_{c,n,j} \cos(2\pi j \frac{t}{T}) + \\ &\sum_{j=1}^{j^*} \theta_{sx,n,j} \sin(2\pi j x_t^*) + \sum_{j=1}^{j^*} \theta_{cx,n,j} \cos(2\pi j x_t^*), \end{aligned} \tag{3}$$

$t = 1, ..., T$ is the linear time trend. In our application, x_t is the NOAA Annual Greenhouse Gas Index (AGGI), x_t^* is the AGGI index re-scaled in the interval $[0, 1]$, i.e., $x_t^* = (x_t - min(x))/(max(x) - min(x))$, θ_0, $\theta_{s,q,j}$, $\theta_{c,q,j}$, $\theta_{sx,q,j}$, $\theta_{cx,q,j}$ are parameters. The MLT component measures the conditional expectation for the indicator $y_{n,t}$, i.e., $m_{n,t} = E[y_{n,t}|I_t]$. Conditioning on AGGI allows to control for the human-made contribution to global warming when modelling the MLT or trend component in a given extreme weather indicator.

The Data Generating Process (DGP) for the MLT (or trend) function is unknown, and approximated, according to the Weierstrass Approximation Theorem, by the trigonometric polynomial specification in (3). In our application, the order of the trigonometric polynomial j^* is fixed in such a way to model fluctuations with periodicity (P^*) larger than 11 years, i.e., $j^* = \lfloor T/P^* \rfloor$, to avoid contamination from the contribution of near periodic natural oscillators, such as the El Niño-Southern Oscillation (ENSO; with periodicity between 2 and 7 years) and the North Atlantic Oscillation (NAO; with variable periodicity) cycles, and from solar activity (with periodicity of about 11 years). This helps to discriminate potential short-term changes in the weather indicators determined by natural phenomena from the more long-term ones determined by human activity. In this respect, we neglect any possible impact of human activity on the natural oscillators themselves, as these are not the object of the current study. Accordingly, as annual data are available over the period 1981-2023, i.e., $T = 43$, we set $j^* = 3$, which yields an MLT component associated with fluctuations with periodicity $P^* = T/j^*$ equal or larger than 14.3 years. Fluctuations with smaller periodicity are then captured by the ST component $s_{n,t} = y_{n,t} - m_{n,t}$, with $E[s_{n,t}|I_t] = 0$.

2.1.1 Empirical implementation

Empirically, the decomposition for the generic climatic indicator y, can be implemented country by country through univariate OLS regression models. For the generic country n it follows the regression model

$$\begin{aligned} y_{n,t} &= \theta_{0,n} + \sum_{j=0.5}^{j^*} \theta_{s,n,j} \sin(2\pi j \frac{t}{T}) + \sum_{j=0.5}^{j^*} \theta_{c,n,j} \cos(2\pi j \frac{t}{T}) + \\ &\sum_{j=0.5}^{j^*} \theta_{sx,n,j} \sin(2\pi j x_t^*) + \sum_{j=0.5}^{j^*} \theta_{cx,n,j} \cos(2\pi j x_t^*) + \varepsilon_{n,t}, \end{aligned} \tag{4}$$

where $\varepsilon_{n,t}$ is i.i.d. with zero mean, variance σ^2, and finite fourth moment, and the regressors $\sin(2\pi j x_t^*)$, $\cos(2\pi j x_t^*)$, $j = 0.5, 1, 2, ..., j^*$, are weakly stationary processes. Under the above conditions, OLS estimation of the model in (4) is consistent and asymptotically normal, using Newey-West standard errors in the case of nonspherical residuals. These results apply straightforwardly in the case the series $y_{n,t}$ is linear or non-linear trend stationary. Even if the conditioning regressor x_t were an I(1) process, its periodic transformation behaves asymptotically as stationary, zero-mean, homoskedastic AR(1) processes. Monte Carlo evidence shows that sine and cosine transforms of a random walk process have strong short-term correlations but not even long memory (see details in Morana, 2024).

Following Muller and Watson (2018), the above decomposition appears to be valid also in the case the series $y_{n,t}$ were an I(1) process. In fact, the model in (3) generalizes

Muller and Watson (2018), as it allows the extraction of the trend/medium to long-term component in the extreme weather indicators of interest by conditioning on information available on potential drivers of their medium to long term evolution, i.e. the series x_t^*. By setting $\theta_{sx,n,j} = \theta_{cx,n,j} = 0$, $j = 0.5, 1, 2, .., j^*$, and noting that

$$\sin(z) = \cos(z - \pi/2), \tag{5}$$

for $z \in [0, 1]$, the model in (3) can be rewritten as a function of cosine terms only, delivering the medium to long-term components of the series of interest as its cosine transform up to order j^* as in Muller and Watson (2018).

The specification allows to assess the anthropogenic contribution to changing extreme weather trend conditions while controlling for non-anthropogenic or natural sources of long term swings in climatic conditions. For instance, a test for a null anthropogenic contribution to evolving climatic conditions for country n involves testing the joint hypothesis H_0: $\theta_{sx,n,j} = \theta_{cx,n,j} = 0$, $j = 1, ..., j^*$ (Test 1). Moreover, a test for the hypothesis of no contribution from natural sources, as for instance from multidecadal oscillators such as the Atlantic Multidecadal Oscillation (AMO), requires testing H_0: $\theta_{s,n,j} = \theta_{c,n,j} = 0$, $j = 1, ..., j^*$ (Test 2). Finally, a test for no evolving climatic conditions requires testing the joint hypothesis H_0: $\theta_{s,n,j} = \theta_{c,n,j} = \theta_{sx,n,j} = \theta_{cx,n,j} = 0$, $j = 1, ..., j^*$ (Test 3).

2.2 The multi-country *MLT-ST* decomposition

The sequential, country-by-country decomposition is empirically straightforward but inefficient, as it does not allow the exploitation of likely commonalities of evolving climatic conditions across European countries. For instance, Cassola et al. (2024) find that the European Extreme Events Climate Index (E3CI) across European countries is well described by four principal components, accounting for about 85% of the total variance. The first PC explains over 50% of the total variance and yields a common European factor. The other factors carry information on excess risk based on geographical location, i.e., Southern vs. Northern Europe excess risk, Atlantic vs. Continental excess risk, and periphery vs. core Europe excess risk.

We can implement a more efficient procedure through an Autometrics panel data estimation procedure. Consider again the generic n, t element in the vector $\mathbf{y}$, i.e., $y_{n,t}$, $n = 1, .., N$, $t = 1, .., T$, yielding the tth period observation for the extreme weather indicator $\mathbf{y}$ for the generic nth country. It follows the panel regression

$$\begin{aligned} y_{n,t} \;=\; & \theta_0 + \sum_{j=0.5}^{j^*} \theta_{s,j} \sin(2\pi j \frac{t}{T}) + \sum_{j=0.5}^{j^*} \theta_{c,j} \cos(2\pi j \frac{t}{T}) + \\ & \sum_{j=0.5}^{j^*} \theta_{sx,j} \sin(2\pi j x_t^*) + \sum_{j=0.5}^{j^*} \theta_{cx,j} \cos(2\pi j x_t^*) + \\ & \sum_{n=1}^{N-1} \theta_{0,n} D_{n,t} + \sum_{n=1}^{N-1} \sum_{j=0.5}^{j^*} \theta_{s,n,j} \sin(2\pi j \frac{t}{T}) D_{n,t} + \sum_{n=1}^{N-1} \sum_{j=0.5}^{j^*} \theta_{c,n,j} \cos(2\pi j \frac{t}{T}) D_{n,t} + \\ & \sum_{n=1}^{N-1} \sum_{j=0.5}^{j^*} \theta_{sx,n,j} \sin(2\pi j x_t^*) D_{n,t} + \sum_{n=1}^{N-1} \sum_{j=0.5}^{j^*} \theta_{cx,n,j} \cos(2\pi j x_t^*) D_{n,t} + \varepsilon_{n,t}, \end{aligned} \tag{6}$$

where $D_{n,t}$ is a dummy variable taking unitary values for country n and zero elsewhere. The first five terms in the regression function, whose marginal effects are measured by

the parameters θ_0, $\theta_{s,j}$, $\theta_{c,j}$, $\theta_{sx,j}$, $\theta_{cx,j}$ yield the common drivers of evolving extreme weather conditions across countries; the remaining elements capture heterogeneities across countries.

The specification in (6) is over profligate and would not be estimable by OLS. For instance, our application, where $N = 40$, $T = 43$, and $j^* = 3$, would require estimating 680 parameters. However, estimation becomes feasible within an Autometrics general-to-specific estimation approach (Hendry et al., 2008). The machine learning procedure allows for efficient model reduction, yielding a final parsimonious econometric model well describing data properties (commonalities and heterogeneity). In the light of Cassola et al. (2024), while some heterogeneity across countries should be expected, we also expect a strong and dominant common component, keeping into account the global nature of climate change. The tests of interest, i.e., Tests 1, 2, and 3 above, can also be implemented within the panel data procedure.

3 The data

We assess the evolution of extreme weather conditions in Europe using the European Extreme Events Climate Index (E3CI) and its seven subcomponents, available for forty European countries monthly since January 1981. The data are available for Albania, Andorra, Austria, Belarus, Belgium, Bosnia-Herzegovina, Bulgaria, Croatia, Cyprus, Czechia, Denmark, Estonia, Finland, France, Germany, Greece, Hungary, Iceland, Ireland, Italy, Latvia, Lithuania, Luxembourg, Malta, Moldova, Montenegro, the Netherlands, North Macedonia, Norway, Poland, Portugal, Romania, Serbia, Slovakia, Slovenia, Spain, Sweden, Switzerland, Ukraine, and the United Kingdom.

The E3CI subcomponents are based on ERA5 atmospheric re-analysis data (https://cds.climate.copernicus.eu/datasets/reanalysis-era5-single-levels?tab=overview) and yield information on seven extreme meteorological events associated with the temporal evolution of extreme maximum and minimum temperatures, precipitation, wind speed, hail, drought, and wildfires. Specifically, the subcomponent indexes yield information on meteorological anomalies as measured by the standardized deviation (z-scores) of monthly figures from their historical mean computed throughout 1981-2010. A larger than unity value reveals excess risk intensity relative to the historical average for any subcomponents. A larger than the unity threshold value, persisting over time and of increasing magnitude, reveals a rising extreme weather risk intensity, i.e., a climatic change that might be caused by global warming.

The overall E3CI index at any time is the simple average of the seven subcomponents, yielding an overall and comprehensive assessment of evolving extreme weather conditions, embedding seven relevant dimensions. Details on the construction of the anomalies are available at https://climateindex.eu/en/the-7-indicators/.

The NOAA Annual Greenhouse Gas Index (AGGI) measures the climate-warming influence of long-lived trace gases in the atmosphere. It is available annually and tracks how GHG's warming influence has changed globally over time. According to the Intergovernmental Panel on Climate Change (IPCC) definition, climate forcing is "An externally imposed perturbation in the radiative energy budget of the Earth's climate system, i.e., through changes in solar radiation, changes in the Earth albedo, or changes in atmospheric gases and aerosol particles." The AGGI tracks changes in the atmospheric global concentration of long-lived, well-mixed greenhouse gases, in particular, carbon dioxide (CO2),

methane (CH4), nitrous oxide (N2O), and halogenated compounds (mainly CFCs). It is available at https://gml.noaa.gov/aggi/aggi.html.

Global warming, i.e., the rise in average temperatures determined by anthropogenic GHG emissions, is one of the most evident consequences of climatic change. It is associated with hot summers and heat waves, mild winters, and various other extreme weather realizations, such as droughts, extreme precipitations and winds, wildfires, and hail, that have intensified in frequency and intensity over time. Extreme heat contributes to increased morbidity and mortality, and it has been of concern in Europe since the early 2000s, especially after the over 70,000 excess deaths registered in summer 2003. In Europe, heat-related deaths were 60,000 in 2022, 47,000 in 2023, and over 40,000 in 2024. (Ballester et al., 2023; García-León et al., 2024). See also https://climate.copernicus.eu/copernicus-summer-2024-hottest-record-globally-and-europe.

On a global scale, the last ten years were the warmest on record, and 2024 was the seventh warmest year. Summer 2024 was the hottest ever measured at 0.76°C above the 1991–2020 average and 1.64°C above the 1850–1900 pre-industrial average. The warming in Europe is almost 1°C higher than the corresponding global increase and higher than in any other continent. In 2022, the average temperature was 2.3°C above the pre-industrial reference value (https://news.un.org/en/story/2023/06/1137867). Extreme weather in Europe is then indicative of changes to come for other continents in scenarios of unabated GHG emissions.

The E3CI index effectively monitors extreme weather realization developments over time, yielding an assessment relative to a historical benchmark referring to the 1980-2010 period. Figure 1 reports average annual figures over the last four decades and the most recent 2020-2023 period for the E3CI index and its subcomponents. The aggregate figures are computed as cross-sectional averages over the forty European countries in the sample. We calculate annual figures by averaging the monthly observations to highlight trend-level changes. The figures reported are rescaled so that values larger than one point to abnormal realizations for the E3CI index and its subcomponents, i.e., to weather conditions more extreme than in the past.

Figure1 here

As shown in Figure 1, the E3CI index points to increased extreme weather realizations over the last fifteen years, which also gets stronger over time. The increase in the index on average since 2020 is even more significant than in the previous decade (2010-2019). The evidence points to worsening weather conditions and extreme events becoming more frequent at the trend level.

From Figure 1, the worsening in average weather conditions detected by the E3CI index can be pinned down to its sources. Extreme-heat developments (max temp) appear to be the most critical driver of the worsening registered by the E3CI index. Extreme heat conditions have been worsening over the last thirty years, pointing to a 25% increase in frequency in the 2000s over the 1990s, then a 60% increase in the 2010s over the 2000s, and a further 20% increase in the last four years in the sample over the previous decade. By comparing current values with those over the 1980s, the increase in extreme heat frequency is over 180%.

Global warming is a two-sided phenomenon. On one side, it leads to hotter summers. On the other hand, it leads to milder winters. The relevance of these implications is evident from Figure 1, where trend developments in extreme-cold realizations (min temp) are reported, too. The overall decrease in the indicator in the most recent period over the 1980s average value is about 30%. The evidence from previous decades shows that these

developments have progressed over time. Therefore, the global warming effect appears asymmetric, leading to more frequent extreme heat episodes than less frequent extreme cold episodes.

Wildfires and drought are also phenomena showing an increasing realization intensity. This finding is consistent with extreme heat developments. The frequency of drought episodes has increased by 30% in the most recent sample relative to the 1980s values. Developments in previous decades were less clear-cut. On the other hand, the frequency of wildfire episodes has been progressive over time. The wildfire indicator points to a 150% frequency increase in the most recent period compared to the 1980s. While the origin of wildfires is most often human-made, their damage depends on their propagation, which depends on weather conditions, especially air humidity and temperatures. In this respect, the global warming effect appears to foster the joint realization of extreme weather events of different types: the frequency increase in drought, wildfire, and heatwave episodes seem to be connected and should be controlled for when evaluating the potential economic damages stemming from global warming.

The frequency of extreme precipitation and wind episodes has also increased over the fifteen years, about 10%-20% relative to the 1980s. The extreme wind frequency increase is more marked in the most recent period (20%) than in the previous decade (10%). On the other hand, the frequency of hail episodes has been decreasing over the last fifteen years. This finding, however, has no implications for hailstorm intensity when they occur. In 2023 and 2024, the size of hailstones has shown to be, on average, bigger than in the past (European Severe Weather Database; https://eswd.eu/cgi-bin/eswd.cgi). In Northern Italy, the probability of hailstones over five centimeters in diameter is currently 300% higher than in the 1980s: in summer 2024, a hailstone with a gigantic diameter of 19 centimeters was registered.

Figure 2 reports the time series for the aggregate European E3CI index and its seven subcomponents. For graphical purposes, we remove the outlying values for the hail data for 1985 and 2022 and replace them with estimated trend values delivered by a structural time series interpolating model.

Figure 2 here

Table 1 reports the results of the Becker et al. (2006) augmented KPSS tests to provide statistical support for the evolving trends noted in the previous descriptive statistics analysis. In particular, we compare results for testing the null hypothesis of level stationarity with the findings obtained for testing the null hypothesis of nonlinear trend stationarity.

Considering the generic time series $\{y_t\}$, the auxiliary model used for testing is

$$y_t = f(t) + \mu_t + \varepsilon_t$$

where $f(t)$ is the purely deterministic component, $\mu_t = \mu_{t-1} + v_t$, $v_t \sim w.n.(0, \sigma_v^2)$, ε_t is an I(0) process potentially heteroskedastic. Under the null hypothesis, $\sigma_v^2 = 0$ and $\mu_t = \mu_0$, yielding level stationarity if

$$f(t) = \theta_0,$$

where θ_0 is a constant term; linear trend stationarity if

$$f(t) = \theta_0 + \theta_1 t,$$

where θ_1 is a parameter and $t = 1, 2, ..., T$ the linear time trend; non-linear trend station-

arity of order r if

$$f(t) = \theta_0 + \sum_{j=1}^{r} \theta_{s,j} \sin(2\pi j \frac{t}{T}) + \sum_{j=1}^{r} \theta_{c,j} \cos(2\pi j \frac{t}{T}),$$

where $\theta_{s,j}$ and $\theta_{c,j}$ are parameters.

The Flexible Fourier form allows for effective modeling of unknown forms of trend developments, accounting for nonlinear and non-monotonous paths over time, as evident from the descriptive trend analysis. Our preferred third-order specification ($r = 3$) allows the trend component to describe fluctuations with periodicity larger than 14 years. This threshold is motivated by climatological arguments concerning the potential drivers of the trend in these series discussed in the previous Section.

TABLE 1 here

As shown in Table 1, the null of level stationarity (column 1) is rejected at the 5% level for the E3CI index and four of its subcomponents, i.e., extreme maximum and minimum temperatures, extreme precipitation, and wildfires. The rejection is at the 1% level for the extreme maximum temperature component, too. On the other hand, the null hypothesis is not rejected for extreme wind, drought, and hail. The null of linear trend stationarity (column 2) is also rejected at the 5% level for the E3CI index and its subcomponents, but the extreme minimum temperature and drought indicators. Rejection at the 1% level is detected for the extreme maximum temperature, precipitation, and wind components. These results suggest that, in general, neither level nor linear trend stationarity well characterize the dynamic properties of the extreme weather series, possibly pointing to more complex forms of non-stationary behavior, in alternative to stochastic non-stationarity. The results reported in Table 1 (columns 3-5) support this view, as the null hypothesis of nonlinear trend stationarity is never rejected even at the 5% level. Two exceptions can be noted for the most profligate third order specification (column 5), i.e., for the E3CI index and its wildfire component, for which non-rejection is only at the 1% level.

These findings are further corroborated by the results of the stationarity test carried out on the country-level individual data reported in Figure 3, showing a widespread rejection of the null hypothesis of level stationarity for any of the indicators and any country, and of the null hypothesis of linear trend stationarity, too. On the other hand, the evidence of nonlinear trend stationarity is never rejected for any country and indicator.

Figure3 here

Hence, significant nonlinear trend developments characterize extreme weather realizations in Europe. Testing the origin of these developments, specifically about global warming and human-made GHG emissions, is the object of the following section. The trend component is also included in Figure 3 for the E3CI index and its components, highlighting the nonlinearity in their temporal evolution, allowing us to dig into their origins and potentially the interconnection between human-made and natural environment contributions.

4 Human-made vs. natural environment climate change drivers

The empirical analysis of extreme weather series trend developments is carried out using the panel data model in (6). OLS estimation is performed through Autometrics, the

automated general-to-specific model reduction strategy by Hendry et al. (2008). The model reduction analysis is carried out for the E3CI index and its seven components, i.e., extreme maximum and minimum temperatures, wind speed, precipitation, droughts, wildfires, and hail, separately. The final econometric models obtained from the reduction analysis are reported in Tables 2 and 3. In particular, in Table 2, we report the final specification for the common components across countries, while in Table 3, the final specification for the components accounting for cross-country heterogeneity. Heteroskedasticity consistent standard errors are reported in all cases.

As shown in Tables 2 and 3, the common component is strongly dominant over the idiosyncratic component, consistent with the global nature of climate change and the potential additional contribution of natural oscillators with long periodicity and global impact. In fact, for the E3CI index and any of its components, the contribution of the Fourier transforms of the GHG emissions index ($x = AGGI$; sx_i, cx_i, $i = 0.5, 1, 2, 3$) and the trigonometric components in the time trend (s_i, c_i, $i = 0.5, 1, 2, 3$) sizably contribute to the modeling of the nonlinear evolution of the underlying dynamics in all cases. No evidence of a dominant impact of any of the two categories over the other can be found. Our framework suggests that trend behavior in the weather series can be attributed partly to human-made GHG emissions and some multidecadal natural oscillators, which might also impact weather behavior at low frequencies. This aligns with previous evidence on global temperatures by Morana and Sbrana (2019).

Not surprisingly, the largest contribution from idiosyncratic sources is detected for the E3CI index, which summarizes the information reported in its components. Nordic countries, i.e., Iceland, Norway, Finland, Sweden, but also Ireland and Switzerland, are pointed as the countries where both the effects of human-driven climate change and multidecadal natural oscillators might have impacted differently than the core group of European countries. The E3CI components can gauge further insights into countries' heterogeneity. For instance, Iceland and Sweden are pointed as outlying countries according to the extreme maximum temperature and wildfire indicators. Iceland was also selected based on the drought component. Norway, Finland, Ireland, and Switzerland are selected according to the wildfire indicator, and Switzerland is also selected according to the extreme precipitation component. Many other countries are pointed as outlying according to one or more other indicator's components. Among the Northern Europeans, Latvia, Estonia, Lithuania; among the Southern Europeans, Malta, Cyprus, Andorra, Greece, Italy, Slovenia, Montenegro, Albania, and North Macedonia. Finally, some evidence of idiosyncratic behavior can also be detected for Czechia, France, and the UK.

In Table 4, we finally report the results of the Wald tests for the null hypothesis of no anthropogenic contribution to trend weather conditions (Test 1), i.e.,

$$H_0 : \theta_{sx,j} = \theta_{sx,n,j} = \theta_{cx,j} = \theta_{cx,n,j} = 0,$$

the null hypothesis of no contribution from natural oscillators (Test 2), i.e.,

$$H_0 : \theta_{s,j} = \theta_{s,n,j} = \theta_{c,j} = \theta_{c,n,j} = 0,$$

and the null hypothesis of non-evolving weather conditions (Test 3), i.e.,

$$H_0 : \theta_{sx,j} = \theta_{sx,n,j} = \theta_{cx,j} = \theta_{cx,n,j} = \theta_{s,j} = \theta_{s,n,j} = \theta_{c,j} = \theta_{c,n,j} = 0,$$

and $j = 0.5, 1, 2, 3$ in all cases.

The results are clear-cut and point to reject the null hypothesis in all cases, supporting the view that underlying or trend weather conditions are evolving and driven by the anthropogenic contribution of GHG emissions and their impact on global warming. They, however, also reflect the impact of multidecadal oscillators such as the Atlantic Multidecadal Oscillation (AMO), which are relevant to shaping weather conditions in Europe.

The trend components reported in Figure 3 are computed by averaging the fitted component delivered by the panel data specification (6). Disentangling the human-made and natural environment contributions does not appear straightforward due to the potential correlation that might affect the two sets of regressors involved, i.e., the transform in AGGI and the transforms in the linear time trend component. Moreover, global warming might also impact the evolution of natural oscillators such as the ENSO and the AMO (Zhiping et al., 2024). Hence, in what follows, we assess the linkages between deteriorating overall trend weather conditions and economic activity.

5 The economic impact of climate change

We assess the economic impact of deteriorating weather conditions within the Growth-at-Risk framework of Adrian et al. (2019) for the forty European countries for which the E3CI extreme weather indicators have been available since 1981. We use real per capita GDP growth data (annual %, constant local currency) from 1981 to 2023. The data are available from the World Bank at https://databank.worldbank.org/metadataglossary/world-development-indicators/series/NY.GDP.PCAP.KD.ZG. Our yearly panel data set is unbalanced, as for some of the post-Soviet countries and East-European countries data are available only for a shorter period. For instance, data for Belarus, Bosnia, Croatia, Czechia, Estonia, Latvia, Lithuania, Moldova, North Macedonia, Poland, Romania, Slovakia, and Slovenia are available since 1991. Data for Montenegro are available since 1998, for Serbia since 1996, and for Ukraine since 1988. In total, our dataset counts 1551 annual observations.

The Growth-at-Risk approach is best suited to measure the effects of tail events, such as extreme weather realizations, on economic activity, yielding insights into their impact on the entire distribution of GDP growth rather than on its mean component only. The approach allows for insights into the effects of extreme weather episodes on downside economic growth risk and potential asymmetries in their economic impact. It allows control of various extreme weather realizations and their joint occurrence. For instance, extreme heat episodes and droughts might create ideal conditions for the spread of wildfires. Therefore, amplification and interaction mechanisms might be controlled within a multivariate specification, allowing for joint conditioning on various E3CI subcomponents.

Our underlying extreme weather measures are conditioned to their potential chief driver, i.e., human-made GHG emissions and their global warming effects, as measured by the AGGI radiative forcing index. We measure these effects through the trigonometric polynomial in the AGGI index. We also allow for the contribution of natural phenomena inducing low-frequency changes in weather conditions, such as the Atlantic Multidecadal Oscillation (AMO). While we do not directly address these potential contributors, we aim to capture their effects through the trigonometric polynomial in the temporal index. Our assessment of the economic impact of extreme weather realizations is consistent with

a "business as usual" GHG growth scenario, as it exploits their current estimated trend.

5.1 Econometric methodology

We implement our Growth-at-Risk analysis within a quantile panel regression with fixed-country effects. The first econometric model assesses the impact of *overall* extreme weather conditions on per capita real GDP growth, allowing for time trend effects and controlling for macro-financial and geopolitical conditions. The baseline regression is

$$\Delta y_{t,j} = \alpha_j + \sum_{s=1}^{2} \gamma_s t^s + \beta E3CI_{t,j} + \sum_{r=1}^{3} \delta_r x_{t,r} + u_{j,t}, \tag{7}$$

where $\Delta y_{t,j}$ is the percent change in the real per capita GDP in period t in country j, $E3CI_{t,j}$ is the E3CI index in period t in country j, α_j is the country fixed effect, and $u_{j,t}$ is an i.i.d. residual. For $s = 1$, t^s is the linear time trend included in the model to capture evolving technical-progress induced underlying GDP growth following Phillipon (2024). For robustness, we also estimate a version of the model allowing for a quadratic linear trend component, i.e., $s = 1, 2$. Finally, $x_{t,r}$, $r = 1, ...3$, are country-invariant conditioning regressors capturing the state of geopolitical conditions, as measured by the Geopolitical Condition Risk Index (GPR, $r = 1$), and overall macro-financial conditions, as proxied by the New CISS Financial Condition Index ($NCISS$, $r = 2$) and the Global Economic Policy Uncertainty Index ($GEPU$, $r = 3$). The New CISS is the equal-weight version of the Composite Indicator of Systemic Stress originally contributed by Hollo et al. (2012). It is comprised of 15 market-based financial stress measures that assess conditions in the financial intermediaries sector, money markets, equity markets, bond markets, and foreign exchange markets. It is available from the ECB at https://data.ecb.europa.eu/data/datasets/CISS/CISS.D.U2.Z0Z.4F.EC.SS_CIN.IDX. The Geopolitical Risk Index is by Caldara and Iacoviello (2021) and yields a worldwide coverage of adverse geopolitical events and tensions. It is available at https://www.matteoiacoviello.com/gpr.htm. The Global Economic Policy Uncertainty Index is available since 1997 at https://www.policyuncertainty.com/index.html. It is a GDP-weighted average of national EPU indices for 21 countries, i.e., Australia, Brazil, Canada, Chile, China, Colombia, France, Germany, Greece, India, Ireland, Italy, Japan, Mexico, the Netherlands, Russia, South Korea, Spain, Sweden, the United Kingdom, and the United States. The missing years 1985-1996 are proxied by the US Economic Policy Uncertainty Index; the years 1981-1984 by the Geopolitical Risk Index. We compute annual figures by averaging monthly observations over the corresponding years. We plot these indicators in Figure 4. In the plots, the gray shades correspond to periods of economic recession, as measured according to the EABCN Eurozone business cycle chronology (https://eabcn.org/dbc/peaksandtroughs/chronology-euro-area-business-cycles). Some association with the state of the business cycle is noticeable for the NCISS and GEPU indicators, which is consistent with their assumed information content.

Our additional econometric models are

$$\Delta y_{t,j} = \alpha_j + \sum_{s=1}^{2} \gamma_s t^s + \beta_i EWI_{i,t,j} + \sum_{r=1}^{3} \delta_r x_{t,j} + u_{j,t} \quad i = 1, ..., 7, \tag{8}$$

$$\Delta y_{t,j} = \alpha_j + \sum_{s=1}^{2} \gamma_s t^s + \sum_{i=1}^{7} \beta_i EWI_{i,t,j} + \sum_{r=1}^{3} \delta_r x_{t,j} + u_{j,t}, \tag{9}$$

where, rather than the composite E3CI index, we use its seven components in the conditioning information set. Hence, $EWI_{i,t,j}$ is the ith E3CI index component in period t in country j. The E3CI index components are the extreme maximum and minimum temperatures, wind speed and precipitation indicators, and the drought, hail, and wildfire components. In regressions (8), we assess the impact of worsening extreme weather conditions by considering each component at the time. In the (9) regression, we jointly assess the impact of all seven E3CI index components. Therefore, our econometric model allows for a richer specification than in previous work, such as Kiley (2024), where the average temperature is the only climatological variable included. As our empirical results show, focusing on a single, yet fundamental, dimension of weather change might lead to an information loss at best and a misspecified growth regression in the worst-case scenario.

Different from classical linear regression analysis, which yields the mean response of the dependent variable to changes in a set of conditioning regressors, quantile regression analysis yields a more flexible alternative, allowing the study of the distributional relationships of variables, i.e., how the various quantiles of the distribution of the dependent variables depend on the realization of the conditioning regressors.

Denoting the cumulative distribution function of the real per capita GDP growth rate in country j in period t conditional on time t information I_t as $G_j(\Delta y_t|I_t)$, its τth conditional quantile is defined

$$Q_{j,t}^{m} = \inf\left\{\Delta y_t : G_j(\Delta y_t|I_t) \geq \tau\right\}, \tag{10}$$

i.e., the minimum value of Δy_t from amongst all those values whose cumulative distribution function value exceeds m, and $\tau = 0.1, 0.2, ..., 0.9$ in our analysis.

The lowest quantile, i.e., $\tau = 0.1$, yields the real per capita GDP growth lower tail outcome, i.e., the smallest value in period t, such that there is a 10% (or greater) probability that the real GDP per capita change will be larger than the value. Symmetrically, the upper quantile, i.e., $\tau = 0.9$, yields the real per capita GDP growth upper tail outcome. The median corresponds to $\tau = 0.5$.

The rationale of quantile regression can be understood by starting with the intuition of ordinary least squares. Given the model

$$y_i = \boldsymbol{\beta}'\mathbf{x}_i + u_i, \tag{11}$$

the least square estimate minimizes the sum of the squared error terms

$$\sum_i (y_i - \hat{\boldsymbol{\beta}}'\mathbf{x}_i)^2. \tag{12}$$

The quantile regression estimate minimizes a weighted sum of the positive and negative error terms

$$\tau \sum_{y_i > \hat{\boldsymbol{\beta}}_\tau'\mathbf{x}_i} \left| y_i - \hat{\boldsymbol{\beta}}_\tau'\mathbf{x}_i \right| + (1-\tau) \sum_{y_i < \hat{\boldsymbol{\beta}}_\tau'\mathbf{x}_i} \left| y_i - \hat{\boldsymbol{\beta}}_\tau'\mathbf{x}_i \right|, \tag{13}$$

where the weight is the τ quantile. The optimization of the loss function in (13) yields an estimated linear relationship between y_i and $\mathbf{x}_i$ where a proportion of data τ $(1-\tau)$ lies above (below) the quantile regression line $\hat{\boldsymbol{\beta}}_\tau'\mathbf{x}_i$. Consistency and asymptotic normality of the quantile regression estimator is established in Koenker and Bassett (1978). For

comparison, we also report results for panel OLS regressions allowing for i) country-fixed effects and ii) country-fixed effects and time-random effects. Some evidence of collinearity dictates the selection of the random-time effects, rather than the fixed-time effects, in our OLS panel regressions. Moreover, we estimated Autometrics OLS panel regressions where the fixed-country and time effects are selected endogenously based on an impulse saturation algorithm (Hendry et al., 2008). As usual in the literature, fixed-country effects in the quantile panel regressions are specified as quantile-invariant.

5.2 Empirical results

Tables 5-8 report the estimation results for the linear time trend models ($s = 1$). Columns 1-3 in each Table report results for the country fixed effects (Least Squares), the country fixed effects plus random time effects panel regressions (Least Squares w/ Time Effects), and the Autometrics panel regressions (Least Squares Autometrics), respectively. Columns 4-12 report results for the quantile panel regressions for the various quantiles $\tau = 0.1, 0.2, ..., 0.9$. In particular, column 8, labeled (5), reports results for the 0.5 quantile, i.e., the median, and therefore for the least absolute deviation regression (MAD). We report robust standard errors in all cases.

Moreover, row 1 in each Table reports the results for the E3CI regressions (7), rows 2-8 the results for the E3CI single components regressions (8), and rows 9-15 the results for the multivariate (9) regressions.

More specifically, the figures reported in Table 5 refer to the estimated β or β_i coefficients measuring the impact of the various extreme weather indicators on the real GDP growth rate. As the climatological variables are z-scores, the reported coefficients measure the real GDP growth rate response per unit of each indicator's Standard Deviation increment. Figures 6-8 report the real GDP growth rate response to the Geopolitical Risk (GPR, δ_1), macro-financial conditions (NCISS, δ_2), and economic policy uncertainty (GEPU, δ_3) control variables, respectively.

For robustness, we report the results obtained from the quadratic trend models ($s = 1, 2$) in Tables A1-A4 in the Appendix.

Table 5 here

Concerning the E3CI regression (7), the evidence is robust to the estimation method and the country and time-fixed effects specification. A comparison between OLS and MAD estimation points to a negative impact of deteriorating weather conditions on economic growth. The point estimates are similar, from -2.4% to -2.7%. The panel quantile regressions show that the negative impact of deteriorating weather conditions on economic growth holds for most of the per capita GDP growth distribution. The downside risk to growth ($\tau = 0.1, 0.2, 0.3$) is much more affected than the central tendency ($\tau = 0.4, 0.5, 0.6$) or upside risk ($\tau = 0.7, 0.8, 0.9$). For instance, the point estimate for the 0.3 quantile (-4.0%) is about fourfold that of the 0.7 quantile (-1.2%). Point estimates for the 0.8 and 0.9 quantiles are insignificant even at the 10% level. The detected asymmetric distributional impact is interesting and deserves further investigation. Hsiang and Jina (2014) show that the state of the business cycle can affect the readiness to invest in a region following a disaster and shape the longer-term recovery of economic activity. A natural disaster can make an ongoing economic contraction more severe due to limited adaptation mechanisms. On the other hand, during expansions, economies can adapt and redirect funds to reconstruct areas hit by those events. See also Kiley (2024).

On average across the 40 countries considered in the study, over the period 1981-2023,

the E3CI index has increased by about 2.7 standard deviations. Hence, the estimated figures convey information on the expected real per capita GDP growth over roughly fifteen years, which yields an expected median contraction in trend real per capita GDP growth of about 0.15% per year over the next fifteen years in a business-as-usual scenario. Given the detected asymmetrical impact, the expected annual impact ranges from -0.08% to -0.25%. Accordig to the EEA assessment, between 1980 and 2023, economic losses caused by climate-related extremes amounted to an estimated EUR 738 billion (2023 prices) in the EU (https://www.eea.europa.eu/en/analysis/indicators/economic-losses-from-climate-related). The average annual (2023 prices) economic losses have increased over time and amount to 8.5 billion in 1980-1989 and 44.5 billion in 2020-2023, i.e., about 0.06% and 0.3% of 2023 EU GDP, respectively. These figures appear to be consistent with our estimated quantile range.

Turning to the single E3CI component regressions (8), we find similar evidence in terms of a negative impact of deteriorating weather conditions on economic growth and a stronger impact on the downside than the upside risk to growth for the extreme maximum temperature and wind indicators, and the droughts and wildfires indicators. Yet, we also find some differences from the baseline regression. For instance, OLS and MAD point estimates are not statistically significant for droughts, even at the 10% level. A significant negative impact can be detected only for the lowest quantiles ($\tau = 0.1, 0.2, 0.3$), from -4.6% to -1.3%. The OLS and MAD point estimates are significant and numerically close for the other three indicators, ranging from -3.7% to -2.9% for extreme wind, -1.2% to -0.7% for wildfires, and -0.6% to -0.5% for extreme maximum temperatures. Yet, while the extreme maximum temperatures and droughts impacts are negative and significant throughout the per capita GDP growth distribution (but for $\tau = 0.9$), for wildfires, the impact is negative and significant only for the lowest and central quantiles. On the other hand, for the extreme minimum temperature and precipitation indicators, the upside risk to growth ($\tau = 0.7, 0.8, 0.9$) is more affected than the central tendency ($\tau = 0.4, 0.5, 0.6$) or the downside risk ($\tau = 0.1, 0.2, 0.3$). For the extreme minimum temperature indicator, the estimates range from -3.1% to -1.3% for the highest quantiles ($\tau = 0.6, 0.7, 0.8, 0.9$) and are not significant otherwise, neither for the MAD nor the OLS regressions. The impact of the extreme precipitation indicator is negative throughout the entire per capita GDP growth distribution but significant over the 0.3 through 0.8 quantile range. In this respect, the point estimates are -2.7% and -3.8% for the 0.3 and 0.7 quantiles, respectively. No significant impact can be found for hail, even at the 10% level, neither for the OLS nor the quantile panel regressions.

The evidence from the joint E3CI components regression (9) is less clear-cut than for the single component regressions. When jointly assessed, all the E3CI components show a negative coefficient in the OLS regressions. Yet, a significant impact (1% level) is found only for the extreme minimum temperature and the hail indicators. The Autometrics OLS panel regression also points to a negative significant impact (at the 10% level) for the extreme maximum temperature and precipitation indicators. On the other hand, the MAD regression points to a negative significant impact (1% level) for the extreme maximum and minimum temperature indicators only. Consistent with the single component regressions, the impact of the extreme minimum temperature indicator is stronger for the highest (-5.5% to -4.0%) than the central (-3.7% to -3.0%) quantiles and not significant for the lowest quantiles ($\tau = 0.1, 0.2$). A negative and significant impact is also found for the extreme maximum temperature indicator for the central part of the per capita GDP distribution only (-1.1% to -0.9%). The negative impact of droughts and wildfires

is only significant for the lowest quantiles (-2.5% to -3.1%, -6.0% to -2.1%). The impact of the extreme precipitation, wind, and hail indicators is negative throughout the per capita GDP distribution. Yet, in general, it is significant only for the lowest and highest quantiles. In this respect, the impact of extreme precipitation on the downside risk to growth is almost double that on the upside risk (-9.7% vs. -4.9%), while for hail the impact is more uniform (-1.9% to -1.5%). The effect is significant for extreme wind only for the highest quantiles (-6% to -3.9%).

By considering again the median point estimates and normalizing their figures to the average time required for a unitary standard deviation change in the indicator of interest from the single (joint) component regressions we find an annual median expected contraction in real per capita GDP growth of about -0.04% (-0.07%) due to increasing maximum temperatures, -0.02% (-0.12%) due to increasing minimum temperatures, -0.14% (-0.11%) due to extreme precipitations, -0.12% (0.01%) due to extreme wind speed, -0.002% (-0.03%) due to droughts, -0.05% (0.03%) due to wildfires, 0.02% (-0.02%) due to hail. The latter figures point to potential bias in growth regressions that neglect interaction across indicators.

Tables 6-8 here

As shown in Tables 6-8, the impact of the conditioning country-invariant macroeconomic, financial, and geopolitical risk regressors is generally negative and significant, consistent with the fact that an increase in these indicators is associated with adverse macroeconomic, financial, or geopolitical developments. In particular, the Geopolitical Risk indicator GPR is significant at the 5% level in all the cases for the Autometrics and MAD models. It is also significant in most cases for the central part of the per capita GDP distribution ($\tau = 0.3, 0.4, 0.5, 0.6, 0.7$). On the other hand, the overall Financial Condition Index $NCISS$ is statistically significant for the highest quantiles regressions ($\tau = 0.8, 0.9$). The Global Economic Policy Uncertainty Index $GEPU$ is significant for all the OLS panel specifications and some of the extreme quantiles regressions ($\tau = 0.1, 0.2, 0.7, 0.8$).

The results are strongly robust to the inclusion of the quadratic trend component. As shown in Table A1, we do not detect any significant changes concerning the impact of the climatological variables on per capita GDP growth, but for one case (E3CI baseline specification, $\tau = 0.7$). Including the quadratic trend makes significant GPR for two more cases for the lowest quantile regressions ($\tau = 0.1, 0.2$) while weakening its significance in one case ($\tau = 0.2$). It also weakens the significance of the $NCISS$ indicator for three cases for the highest quantile regressions ($\tau = 0.8, 0.9$). Including the quadratic trend appears to be a substitute for $GEPU$, which is mainly insignificant across various specifications. This latter finding is consistent with results in the literature suggesting that including a quadratic trend helps to control for fixed-time effects (Tables A2-A4).

6 Conclusions

It is now widely acknowledged that human activities have been responsible for Earth's warming since the Industrial Revolution, i.e., Global Warming. As Earth's climate has warmed, more frequent and intense extreme weather episodes have been observed worldwide, such as heat waves, drought, wildfires, floods, snowstorms, hail, and hurricanes. These phenomena will worsen in a warming climate, yielding economic, financial, and human costs. In this respect, Europe is warming faster than the global average and will

continue to do so throughout this century. The mean annual temperature over European land areas in the last decade was 2.12 to 2.19^{o}C warmer than during the pre-industrial period, already higher than the Paris Agreement target. Without further mitigation policies, land temperatures in Europe are projected to increase further by 1.2 to 3.4^{o}C under the SSP1-2.6 scenario and by 4.1 to 8.5^{o}C under the SSP5-8.5 scenario (by 2071-2100, compared to 1981-2010). The highest level of warming is projected across north-eastern Europe, northern Scandinavia, and inland areas of Mediterranean countries. The lowest warming is expected in Western Europe, especially in the United Kingdom, Ireland, western France, Benelux countries, and Denmark (EEA, 2024). In light of the above evidence, this paper focuses on Europe and yields two original contributions. First, building on Morana (2024) and Morana and Sbrana (2019), we assess the linkage between anthropogenic GHG emissions and underlying extreme weather conditions using an innovative panel regression trend-cycle decomposition approach. The analysis is based on the European Extreme Events Climate Index (E3CI) and its seven subcomponents, i.e., extreme maximum and minimum temperatures, wind speed, precipitation, droughts, wildfires, and hail, available for 40 European countries since 1981. To the authors' knowledge, this is the first study to investigate such a detailed dataset. The approach accounts for the human-made contribution, as measured by changes in the atmospheric global GHG concentrations of GHG, as well as of natural phenomena, to evolving weather conditions. It allows for potential unknown nonlinearities in the relationship between extreme weather and its drivers. It also accounts for cross-countries potential commonalities and heterogeneity, as climate change is a global externality, i.e., one country's emissions affect all countries by adding to the GHG stock in the Earth's atmosphere, from which extreme weather episodes might increase in frequency and intensity. Our findings support the evidence on the contribution of human-made GHG emissions to the deterioration of underlying extreme weather conditions and their highly nonlinear pattern. Consistent with the global nature of climate change and the additional contribution of natural oscillators with long periodicity and global impact, we also point to a dominant common over idiosyncratic component. This finding aligns with Bilal and Kanzig (2024).

We exploit the above findings and assess the economic impact of the multifaceted dimensions of underlying deteriorating weather conditions, focusing on GDP growth dynamics and the 40 European countries for which the E3CI index and its components are available. We conduct our Growth-at-Risk analysis within a quantile panel regression framework, which is best suited to measure the effects of tail events, such as extreme weather realizations, yielding insights into their impact on the entire distribution of GDP growth rather than on its mean component only. It allows for the uncovering of potential distributional asymmetries in their economic impact. Our empirical findings support these nonlinearities. For instance, our baseline regressions assessing the impact of deteriorating overall extreme weather conditions, as measured by the E3CI index, show that their negative impact holds through the GDP growth rate distribution. Yet the effect on the lowest quantiles of GDP growth is about fourfold that of the highest quantiles. The results of the single E3CI component regressions also show the downside risk to growth being stronger than the upside risk for various factors, such as rising extreme maximum temperature, wind speed, drought, and wildfire indicators. Albeit less clear-cut, the negative economic impact of worsening extreme weather conditions in Europe is also confirmed when the E3CI subcomponents are jointly assessed. Under a business-as-usual scenario, extreme weather episodes might generate a median contraction in trend real per capita GDP growth of about -0.15%.per year.

Worsening weather conditions is a multifaceted phenomenon. Overall, our findings point to the relevance of directly considering other dimensions beyond the impact of rising temperatures and accounting for their interactions in growth regressions. However, more research is needed to pin down the transmission mechanism of these adverse climatological developments. Recent discussions on the aggregate demand channels in Usman et al. (2024), Natoli (2023), and Ciccarelli and Marotta (2024) are surely of interest in this respect.

7 Appendix

Tables A1-A4 here

References

[1] Adrian, T., Boyarchenko, N., Giannone, D., 2019. Vulnerable growth. American Economic Review 109, 1263-1289.

[2] Auffhammer, M., 2018. Quantifying economic damages from climate change. Journal of Economic Perspectives 32, 33-52.

[3] Ballester, J., Quijal-Zamorano, M., Méndez Turrubiates, R.F., Pegenaute, F., Herrmann, F.R., Robine J.M., Basagaña, X., Tonne, C., Antó, J.M., Achebak, H., 2023. Heat-related mortality in Europe during the summer of 2022. Nature Medicine 29, 1857-1866.

[4] Becker, R., Enders, W., Lee, J., 2006. A stationarity test in the presence of an unknown number of smooth breaks. Journal of Time Series Analysis 27, 381-409.

[5] Bilal, A., Kanzig, D. R., 2024. The macroeconomic impact of climate change: Global vs. local temperature. National Bureau of Economic Research Working Paper, no. 32450.

[6] Caldara, D., Iacoviello, M., 2021, Measuring geopolitical risk, working paper, Board of Governors of the Federal Reserve Board, November 2021.

[7] Cassola, N., Morana, C., Ossola, E., 2024. Climate change risk pricing in the European stock market. Applied Economics. Forthcoming.

[8] Ciccarelli, M., Marotta, F., 2024. Demand or supply? An empirical exploration of the effects of climate change on the macroeconomy. Energy Economics, 129, 107-163.

[9] EEA, 2024. Global and European temperatures. Available at https://www.eea.europa.eu/en/analysis/indicators/global-and-european-temperatures

[10] Felbermayr, G., Groschl, J., 2014. Naturally negative: The growth effects of natural disasters. Journal of Development Economics 111, 92-106.

[11] García-León, D., Masselot, P., Mistry, M.N., Gasparrini, A., Motta, C., Feyen, L., Ciscar, J.-C., 2024. Temperature-related mortality burden and projected change in 1368 European regions: a modelling study. Lancet Public Health 9, 644–653.

[12] Hendry, D.F., Johansen, S., Santos, C., 2008. Automatic selection of indicators in a fully saturated regression. Computational Statistics 33, 317-335.

[13] Hollo, D., Kremer, M, Lo Duca, M., 2012. CISS - a composite indicator of systemic stress in the financial system. European Central Bank Working Paper, No. 1426.

[14] Hsiang, S.M., Jina, A.S., 2014. The causal effect of environmental catastrophe on long-run economic growth: Evidence from 6,700 cyclones. National Bureau of Economic Research Working Paper Series, no. 20352.

[15] Kahn, M. E., Mohaddes, K., Ng, R. N., Pesaran, M. H., Raissi, M., Yang, J.-C., 2021. Long-term macroeconomic effects of climate change: A cross-country analysis. Energy Economics 104, 105-624.

[16] Kiley, M.T., 2024. Growth at risk from climate change, Economic Inquiry 62, 1134-1151.

[17] Koenker, R., Bassett, G., 1978. Regression quantiles. Econometrica 46, 33-50.

[18] Kotz, M., Levermann, A., Wenz, L., 2022. The effect of rainfall changes on economic production. Nature 601, 223–227.

[19] Kotz, M., Wenz, L., Stechemesser, A., Kalkuhl, M., Levermann, A., 2021. Day-to-day temperature variability reduces economic growth. Nature Climate Change 11, 319-325.

[20] Morana, C., Sbrana, G., 2019. Climate change implications for the catastrophe bonds market: An empirical analysis. Economic Modelling 81, 274-294.

[21] Morana, C., 2024. A new macro-financial condition index for the euro area. Econometrics and Statistics 29, 64-87.

[22] Moore, F. C., Drupp, M. A., Rising, J., Dietz, S., Rudik, I., Wagner, G., 2024. Synthesis of evidence yields high social cost of carbon due to structural model variation and uncertainties. National Bureau for Economic Research Working Papers Series, no. 32544.

[23] Muller, U., Watson, M., 2018. Long-Run Covariability, Econometrica 86, 775-804.

[24] National Academies of Sciences, 2020. Climate change: Evidence and causes. Update 2020. The National Academies Press, Washington, DC, p. B-2. doi:10.17226/25733.

[25] Natoli, F., 2023. The macroeconomic effects of temperature surprise shocks. Bank of Italy Temi di Discussione (Working Paper), no. 1407.

[26] Noy, I., 2009. The macroeconomic consequences of disasters. Journal of Development Economics 88, 221-231.

[27] Philippon, T., 2022. Additive growth. National Bureau for Economic Research Working Papers Series, no. 29950.

[28] Usman, S., Fernandez, G. G.T., Parker, M., 2024. Going NUTS: the regional impact of extreme climate events over the medium term. European Central Bank Working Paper, no 3002.

[29] Zhiping C., Li, L., Wang, B., Fan, J., Lu, T., Lv, K., 2024. The impact of global warming on ENSO from the perspective of objective signals. Atmospheric Research 299.

Figure 1: Extreme weather events in Europe

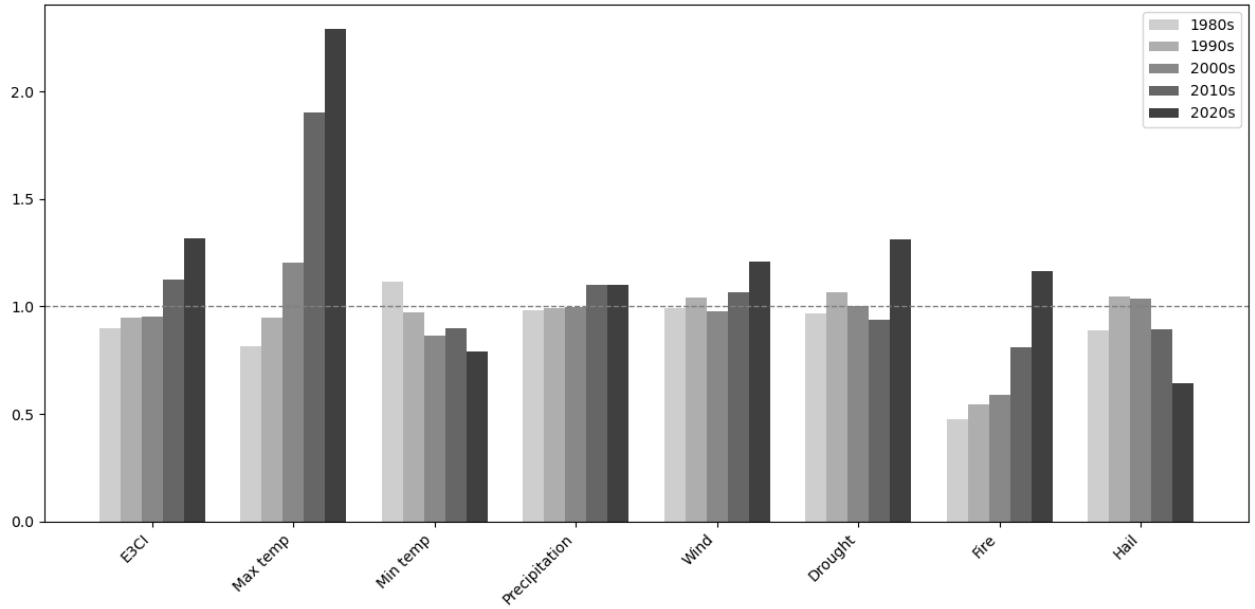

Note: This figure reports average annual values over the last four decades and the most recent 2020-2023 period for the E3CI index and its subcomponents. The aggregate values are computed as cross-sectional averages over the forty European countries in the sample. The values reported are rescaled such that values larger than one point to abnormal realizations for the E3CI index and its subcomponents, i.e., to weather conditions more extreme than in the past.

Figure 2: Evolving extreme weather conditions in Europe

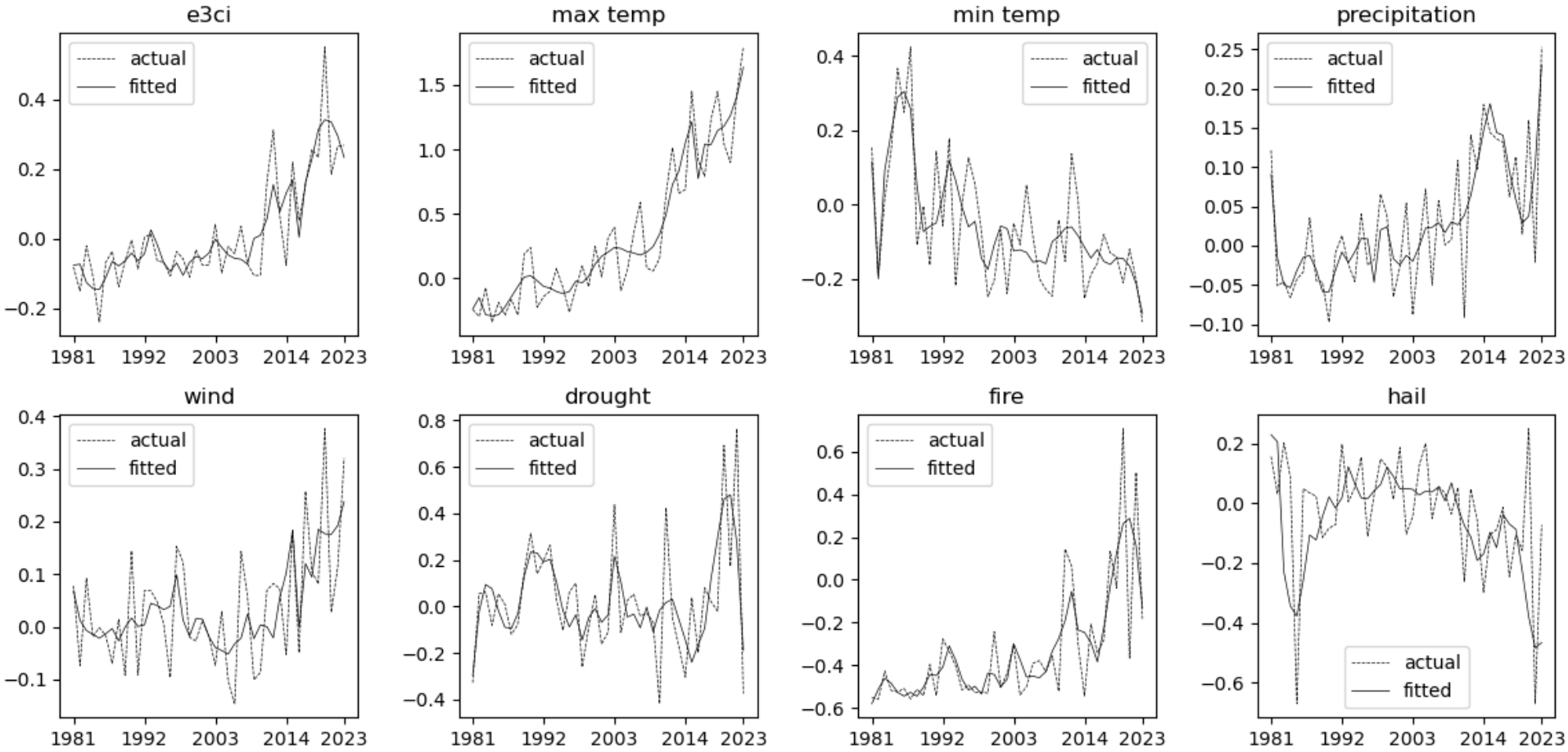

Note: This figure reports the time series for the actual values and their fitted trend components for the aggregate European E3CI index and its seven subcomponents for the period 1981-2023. The aggregate values are computed as cross-sectional averages over the forty European countries in the sample.

Figure 3: Stationarity tests for the extreme weather indicators across countries

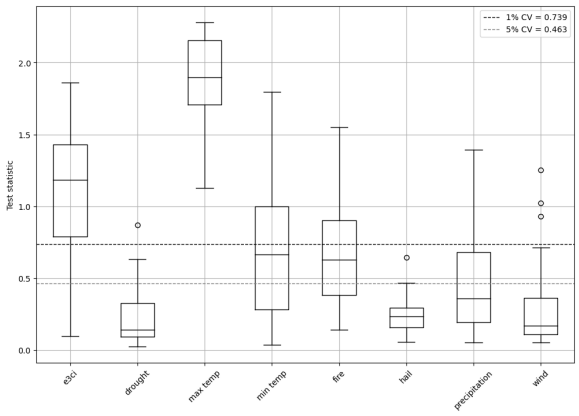

(a) level

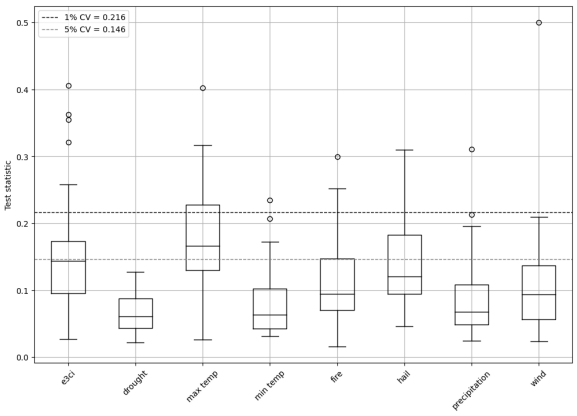

(b) linear trend

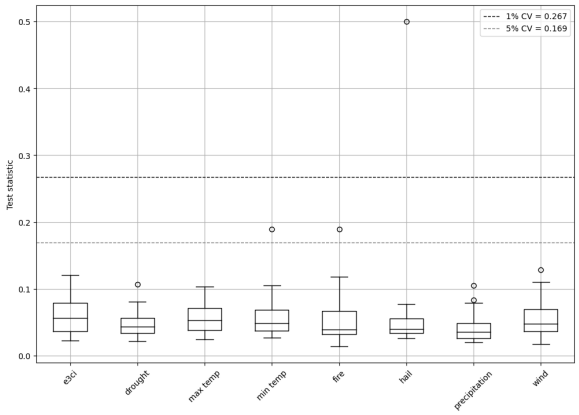

(c) first-order nonlinear trend

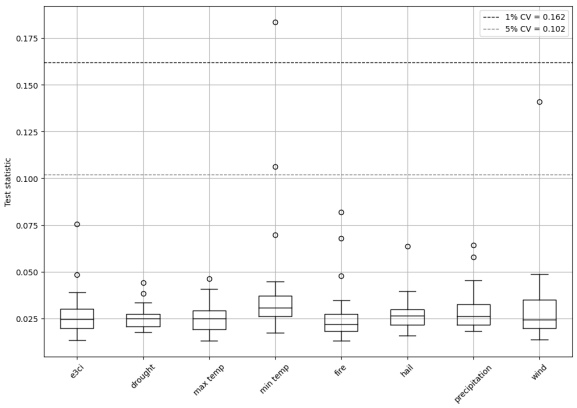

(d) second-order nonlinear trend

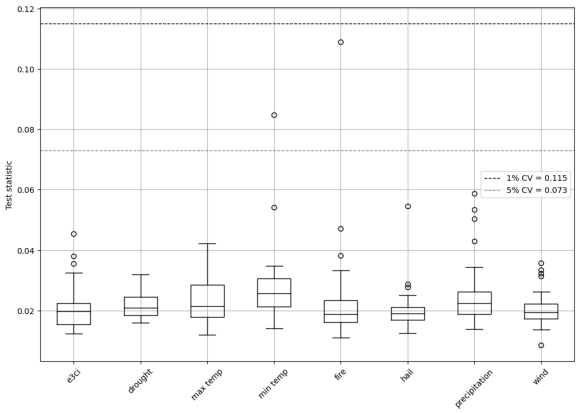

(e) third-order nonlinear trend

Note: This figure reports the results of the Becker et al. (2006) stationarity tests carried out on the country-level E3CI index and its seven subcomponents for the period 1981-2023.

Figure 4: Macro-financial and geopolitical risk indicators

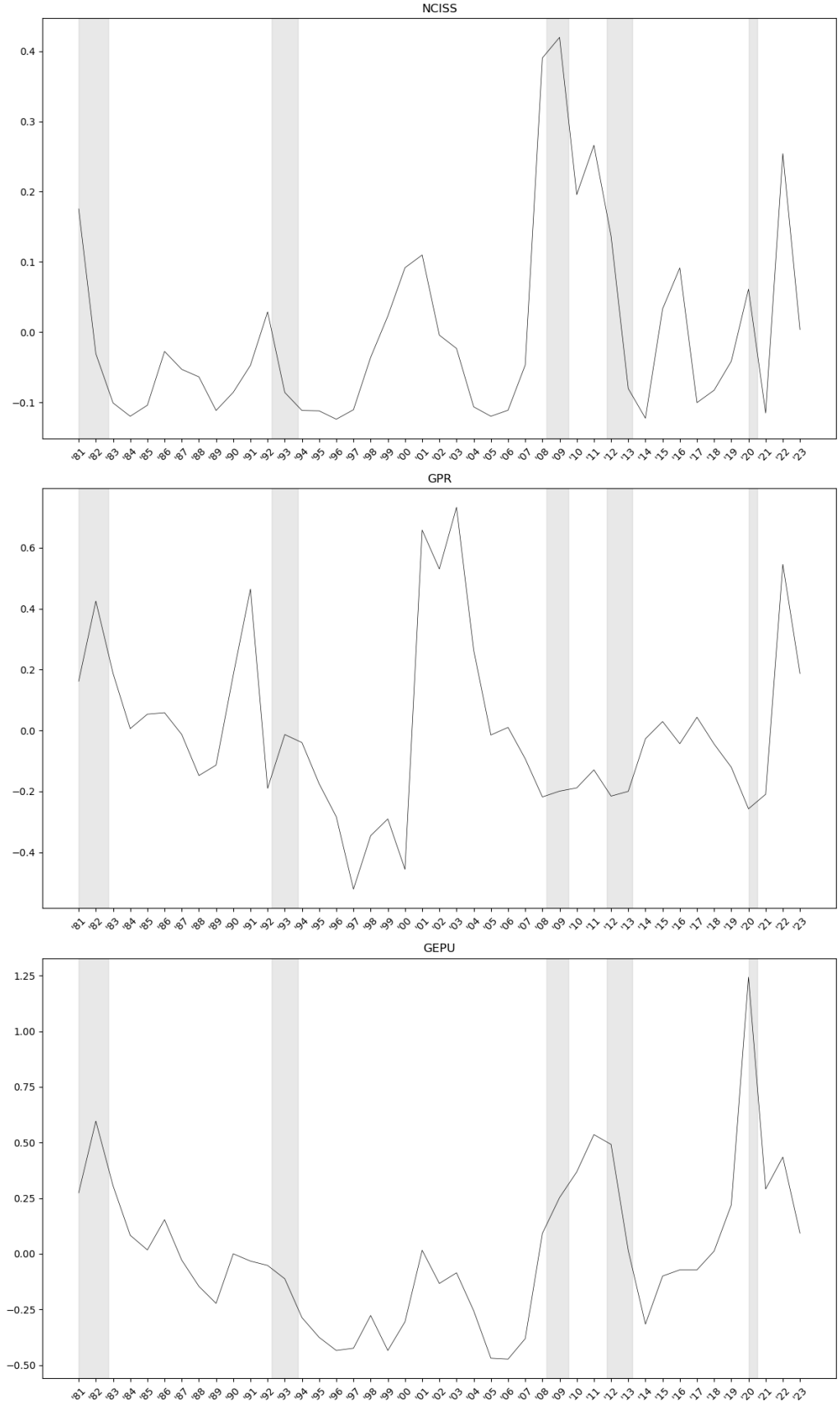

Note: This figure reports the time series for the NCISS, GPR, and GEPU indices for the period 1981-2023, with recessions in the Euro area shaded in grey.

Table 1: Stationarity tests for the extreme weather indicators for Europe (average)

	level	linear trend	first-order nonlinear trend	second-order nonlinear trend	third-order nonlinear trend
E3CI	0.649	0.177	0.137	0.087	0.083
Max temp	0.754	0.219	0.094	0.078	0.073
Min temp	0.624	0.098	0.073	0.042	0.043
Precipitation	0.576	0.452	0.047	0.052	0.032
Wind	0.388	0.233	0.089	0.056	0.062
Drought	0.113	0.100	0.104	0.040	0.037
Fire	0.637	0.159	0.112	0.084	0.109
Hail	0.260	0.155	0.067	0.059	0.059
C.V. 1%	0.739	0.216	0.267	0.162	0.115
C.V. 5%	0.463	0.146	0.169	0.102	0.073

This table reports the results of the Becker et al. (2006) stationarity tests for the average European values of the E3CI index and its subcomponents. The average values are computed as cross-sectional averages over the forty European countries in the sample.

Table 2: Common drivers of evolving extreme weather conditions across countries

	Dependent variable							
	E3CI	Max temp	Min temp	Precipitation	Wind	Drought	Fire	Hail
Psx05	2.677	-2.437	38.679	-	24.554	-	-	-21.780
	(0.992)	(0.569)	(4.342)		(6.043)			(3.783)
Psx1	-2.616	-6.180	0.115	-	-7.239	-	0.392	-
	(0.606)	(1.163)	(0.045)		(1.867)		(0.059)	
Psx2	0.343	-0.382	-	-	-1.628	1.438	1.909	-
	(0.151)	(0.137)			(0.457)	(0.285)	(0.324)	
Psx3	-0.269	-	-	0.133	-0.165	-0.365	-0.402	-0.403
	(0.052)			(0.023)	(0.063)	(0.051)	(0.066)	(0.078)
Pcx05	5.903	10.129	2.704	-	9.387	-5.430	-	4.164
	(1.122)	(2.178)	(0.467)		(2.192)	(0.872)		(0.574)
Pcx1	-	-3.644	15.901	-0.748	9.228	2.770	-	-9.400
		(0.734)	(1.692)	(0.122)	(2.428)	(0.225)		(1.429)
Pcx2	0.089	-1.452	2.215	-	-	-	0.539	-
	(0.029)	(0.252)	(0.232)				(0.092)	
Pcx3	0.151	-	0.284	-0.231	-	1.133	0.712	-0.424
	(0.035)		(0.053)	(0.043)		(0.101)	(0.112)	(0.086)
Ps05	-2.825	-	-41.655	-1.825	-28.299	6.607	3.718	21.132
	(0.986)		(4.801)	(0.286)	(6.897)	(0.540)	(0.719)	(3.852)
Ps1	3.022	6.869	-	-	7.432	-	-	-
	(0.640)	(1.234)			(1.886)			
Ps2	-0.326	0.649	-	-	1.905	-1.347	-1.990	-0.322
	(0.164)	(0.174)			(0.538)	(0.280)	(0.334)	(0.038)
Ps3	0.107	-	-	-0.102	0.326	-	-	0.231
	(0.048)			(0.022)	(0.098)			(0.061)
Pc05	-6.073	-11.056	-2.499	-0.078	-9.464	5.358	-0.224	-3.796
	(1.118)	(2.188)	(0.482)	(0.008)	(2.192)	(0.863)	(0.044)	(0.536)
Pc1	-	2.675	-17.154	-	-11.006	-	1.731	9.215
		(0.823)	(1.904)		(2.851)		(0.320)	(1.454)
Pc2	-	1.439	-2.690	-0.160	-0.450	0.662	-	-
		(0.192)	(0.275)	(0.024)	(0.124)	(0.054)		
Pc3	-0.194	-	-0.499	0.158	-	-0.851	-0.638	0.211
	(0.036)		(0.059)	(0.033)		(0.088)	(0.103)	(0.069)
Constant	0.046	1.690	1.851	1.138	2.386	-3.958	-2.606	0.282
	(0.035)	(0.401)	(0.336)	(0.173)	(0.565)	(0.325)	(0.453)	(0.154)
R^2	0.381	0.601	0.278	0.117	0.093	0.150	0.323	0.169
$\bar{R}^2$	0.372	0.598	0.270	0.109	0.083	0.142	0.315	0.164

This table reports the regression coefficients for the common components across countries of the panel data model in (6). OLS estimation is performed through Autometrics, the automated general-to-specific model reduction strategy by Hendry et al. (2008). The model reduction analysis is carried out for the E3CI index and for each of its components separately. Heteroskedasticity-consistent standard errors are shown in parentheses.

Table 3: Heterogeneities of evolving extreme weather conditions across countries

Dependent variable												
E3CI		Max temp		Min temp		Precipitation		Wind		Drought		Fire	
Pcos05xIS	0.174	Pcos05tMT	-0.294	Psin3xAL	-0.171	Psin1xLT	0.137	Psin3xSI	0.138	Psin1tIT	0.205	Psin05tIE	-0.685
	(0.026)		(0.136)		(0.060)		0.043		(0.053)		(0.082)		(0.095)
Pcos05xIE	0.107	Pcos05tSI	-0.347	Psin3xMK	-0.117	Psin1xLU	0.126	Pcos05xCY	-0.097	Psin1tMK	0.247	Psin05tMT	0.383
	(0.039)		(0.118)		(0.049)		0.034		(0.048)		(0.110)		(0.080)
Pcos05xNO	0.115	Pcos05tSE	0.223	Pcos05xLV	-0.132	Pcos05xFR	0.083	Pcos05xEL	-0.098	Psin3tIS	0.237	PintAD	-0.344
	(0.030)		(0.089)		(0.051)		0.026		(0.034)		(0.082)		(0.047)
Psin05tAT	-0.076	Pcos1tIS	-0.325	Psin05tLV	0.101	Pcos05xMT	0.134	Pcos05xMK	-0.115	Pcos05tAL	0.280	PintAT	-0.354
	(0.025)		(0.088)		(0.043)		0.074		(0.048)		(0.097)		(0.043)
Pcos05tFI	0.114			Pcos05tCY	0.195	Pcos05xCH	0.114	Pcos2xUK	-0.122	Pcos05tEL	0.223	PintEE	-0.273
	(0.036)				(0.076)		0.037		(0.047)		(0.080)		(0.046)
Pcos05tSE	0.113			Pcos05tEE	-0.120	Pcos1xLU	0.099	Pcos1tCZ	-0.128	Pcos05tME	0.183	PintFI	-0.331
	(0.029)				(0.052)		(0.051)		(0.059)		(0.092)		(0.040)
Psin05tCH	-0.109			Pcos1tUK	0.100	Psin1tMK	-0.088					PintIS	-0.716
	(0.022)				(0.041)		(0.041)						(0.036)
PintFI	-0.092					Psin3tLU	0.101					PintNO	-0.524
	(0.023)						(0.040)						(0.030)
PintIS	-0.163											PintSE	-0.350
	(0.016)												(0.035)
PintIE	-0.127											PintCH	-0.543
	(0.022)												(0.041)
PintNO	-0.109											PintUK	-0.352
	(0.017)												(0.052)
PintSE	-0.083												
	0.019												

This table reports the regression coefficients for the components accounting for cross-country heterogeneity of the panel data model in (6). OLS estimation is performed through Autometrics, the automated general-to-specific model reduction strategy by Hendry et al. (2008). The model reduction analysis is carried out for the E3CI index and for each of its components separately. Heteroskedasticity-consistent standard errors are shown in parentheses.

Table 4: Wald tests

	Test 1	Test 2	Test 3
E3CI	10.978 [0.000]	12.224 [0.000]	26.789 [0.000]
	F(10,1694)	F(10,1694)	F(20,1694)
Max temp	18.363 [0.000]	15.055 [0.000]	128.28 [0.000]
	F(6,1704)	F(9,1704)	F(15,1704)
Min temp	23.746 [0.000]	23.3 [0.000]	32.819 [0.000]
	F(9,1701)	F(9,1701)	F(18,1701)
Precipitation	10.168 [0.000]	28.743 [0.000]	12.849 [0.000]
	F(9,1703)	F(7,1703)	F(16,1703)
Wind	4.9724 [0.000]	3.9944 [0.000]	8.1602 [0.000]
	F(11,1700)	F(8,1700)	F(19,1700)
Drought	48.223 [0.000]	17.192 [0.000]	17.645 [0.000]
	F(5,1703)	F(11,1703)	F(16,1703)
Fire	12.142 [0.000]	37.595 [0.000]	47.76 [0.000]
	F(5,1698)	F(7,1698)	F(21,1698)
Hail	15.822 [0.000]	14.749 [0.000]	20.475 [0.000]
	F(5,1708)	F(6,1708)	F(11,1708)

This table reports the results of the Wald tests for the null hypothesis of no anthropogenic contribution to evolving extreme weather conditions (Test 1), of no contribution from natural sources (Test 2), and of no evolving extreme weather conditions (Test 3).

Table 5: Economic impact of extreme weather events, linear trend specification

	Least Squares	Least Squares w/ time effects	Least Squares Autometrics	(1)	(2)	(3)	(4)	(5)	(6)	(7)	(8)	(9)
Single-component models												
E3CI	-2.649***	-2.559***	-2.246***	-8.658***	-5.491***	-3.989***	-2.864***	-2.337***	-1.743**	-1.186*	-0.280	1.054
	(0.737)	(0.737)	(0.711)	(1.480)	(1.226)	(1.102)	(0.795)	(0.660)	(0.706)	(0.705)	(0.777)	(0.971)
Max temp	-0.463**	-0.436**	-0.450***	-1.198***	-0.618**	-0.569***	-0.555***	-0.607***	-0.474***	-0.375**	-0.185	0.180
	(0.198)	(0.198)	(0.175)	(0.419)	(0.272)	(0.203)	(0.165)	(0.158)	(0.180)	(0.187)	(0.229)	(0.281)
Min temp	-0.908	-1.026	-0.720	2.747	0.968	-0.452	-0.194	-0.443	-1.253**	-1.414**	-1.293*	-3.105***
	(0.797)	(0.800)	(0.590)	(2.153)	(0.860)	(0.697)	(0.654)	(0.604)	(0.572)	(0.623)	(0.771)	(0.911)
Drought	-0.821	-0.767	0.225	-4.567***	-2.921***	-1.344*	-0.231	-0.067	1.082*	1.081*	1.780**	2.621***
	(0.555)	(0.554)	(0.551)	(0.945)	(0.617)	(0.760)	(0.594)	(0.635)	(0.596)	(0.574)	(0.702)	(1.014)
Wind	-3.391***	-3.408***	-2.874***	-7.158**	-4.952**	-4.314***	-3.316***	-3.637***	-2.310**	-2.779**	-2.251*	-1.448
	(1.203)	(1.202)	(1.083)	(3.115)	(2.023)	(1.441)	(0.963)	(0.877)	(1.017)	(1.128)	(1.201)	(1.848)
Precipitation	-2.722*	-2.560*	-3.849***	-0.287	-1.544	-2.747**	-3.401***	-4.260***	-4.427***	-3.803***	-4.720***	-3.209
	(1.395)	(1.390)	(1.116)	(4.345)	(1.691)	(1.222)	(1.079)	(1.027)	(1.059)	(1.116)	(1.346)	(2.617)
Fire	-1.206***	-1.156***	-0.698*	-5.249***	-3.238***	-2.181***	-1.083**	-1.011**	-0.291	-0.027	0.552	0.779*
	(0.407)	(0.406)	(0.408)	(0.677)	(0.593)	(0.668)	(0.453)	(0.396)	(0.448)	(0.415)	(0.415)	(0.430)
Hail	0.461	0.420	0.204	1.642	0.485	0.700	0.871	1.120*	0.654	0.311	-0.070	-0.487
	(0.601)	(0.601)	(0.546)	(1.223)	(0.704)	(0.690)	(0.602)	(0.589)	(0.606)	(0.566)	(0.681)	(0.872)
Multi-component model												
Max temp	-0.591	-0.570	-0.823*	1.451	0.294	-0.459	-0.882**	-1.092**	-1.105**	-1.074**	-0.983	-0.474
	(0.567)	(0.568)	(0.468)	(0.949)	(0.546)	(0.490)	(0.440)	(0.437)	(0.447)	(0.512)	(0.739)	(0.892)
Min temp	-3.959***	-4.027***	-3.697***	0.157	-1.939	-3.119***	-3.033***	-3.023***	-3.658***	-4.199***	-4.018***	-5.544***
	(1.125)	(1.130)	(0.926)	(2.127)	(1.224)	(0.967)	(0.932)	(0.959)	(1.003)	(1.092)	(1.482)	(1.659)
Drought	-0.955	-0.874	-0.770	-2.806*	-3.090***	-2.454**	-1.088	-0.947	-0.424	-0.075	-0.159	1.413
	(0.878)	(0.876)	(0.809)	(1.657)	(1.180)	(1.041)	(0.887)	(0.787)	(0.763)	(0.744)	(1.009)	(1.527)
Wind	-1.618	-1.927	-0.873	-0.815	-1.449	-2.007	-0.806	0.215	0.686	-1.233	-3.831*	-6.038*
	(1.826)	(1.824)	(1.415)	(3.182)	(2.463)	(1.722)	(1.389)	(1.330)	(1.302)	(1.524)	(2.086)	(3.562)
Precipitation	-3.026	-2.778	-3.794*	-9.661**	-8.499**	-3.873	-2.878	-3.391	-3.102	-2.689	-2.961	-4.867*
	(2.593)	(2.593)	(2.150)	(4.258)	(3.418)	(2.605)	(2.166)	(2.076)	(1.931)	(2.036)	(2.551)	(2.832)
Fire	-0.745	-0.744	-0.109	-6.120***	-2.145**	-0.648	0.146	0.577	0.811	0.978	1.741*	1.380
	(0.765)	(0.763)	(0.684)	(1.415)	(0.864)	(0.834)	(0.672)	(0.660)	(0.640)	(0.667)	(0.976)	(1.270)
Hail	-2.144***	-2.163***	-1.944***	-1.658	-1.847*	-0.932	-1.177	-1.062	-1.467**	-1.813**	-1.616	-1.084
	(0.829)	(0.832)	(0.665)	(1.416)	(0.955)	(0.806)	(0.733)	(0.739)	(0.738)	(0.750)	(1.045)	(1.574)

This table reports the regression coefficients obtained from regressing real GDP per capita growth on the E3CI index and its subcomponents. Single-component models report the regression coefficients obtained from regressing real GDP per capita growth on the E3CI index and its subcomponents, separately (one at a time). Multi-component model reports the regression coefficients obtained from a multivariate regression of real GDP per capita growth on the E3CI index subcomponents. These regressions contain a linear time trend and the additional control variables NCISS, GPR, and GEPU. The first column reports OLS coefficients with country fixed effects. The second column reports OLS coefficients with country fixed effects and time random effects. Period weights (PCSE) standard errors are shown in parentheses in both columns. The third column reports OLS coefficients using Autometrics panel regressions. Heteroskedasticity-consistent (HCSE) standard errors are shown in parentheses. Columns (1)-(9) refer to quantile regression of the related decile, e.g., (5) refers to 0.5 quantile/median regression. *, **, and *** denote statistical significance at the 10%, 5%, and 1% level, respectively.

Table 6: GPR coefficients, linear trend specification

	Least Squares	Least Squares w/ time effects	Least Squares Autometrics	(1)	(2)	(3)	(4)	(5)	(6)	(7)	(8)	(9)
Single-component model with												
E3CI	-0.554	-0.561	-0.646**	-1.344	-0.861	-0.787**	-0.697**	-0.576**	-0.586**	-0.710**	-0.386	0.271
	(0.361)	(0.455)	(0.306)	(0.934)	(0.567)	(0.333)	(0.292)	(0.278)	(0.281)	(0.286)	(0.379)	(0.526)
Max temp	-0.548	-0.556	-0.668**	-1.518	-1.035*	-0.667*	-0.505*	-0.559**	-0.560**	-0.654**	-0.334	0.274
	(0.361)	(0.454)	(0.302)	(1.110)	(0.567)	(0.341)	(0.289)	(0.273)	(0.273)	(0.288)	(0.387)	(0.519)
Min temp	-0.559	-0.569	-0.798***	-1.536	-0.835	-0.631*	-0.463	-0.468*	-0.784***	-0.884***	-0.558	0.283
	(0.363)	(0.473)	(0.301)	(1.808)	(0.538)	(0.354)	(0.304)	(0.266)	(0.267)	(0.271)	(0.345)	(0.615)
Drought	-0.544	-0.553	-0.708**	-1.579	-0.436	-0.532	-0.480	-0.589**	-0.729***	-0.852***	-0.236	0.493
	(0.362)	(0.466)	(0.306)	(1.241)	(0.435)	(0.350)	(0.305)	(0.269)	(0.265)	(0.279)	(0.388)	(0.481)
Wind	-0.550	-0.560	-0.677**	-1.461	-0.712	-0.639*	-0.631**	-0.551**	-0.598**	-0.595**	-0.300	0.152
	(0.361)	(0.477)	(0.302)	(1.265)	(0.441)	(0.351)	(0.292)	(0.280)	(0.280)	(0.300)	(0.375)	(0.502)
Precipitation	-0.552	-0.560	-0.731**	-1.347	-0.683	-0.871**	-0.529*	-0.604**	-0.552**	-0.721**	-0.412	0.104
	(0.361)	(0.449)	(0.303)	(1.507)	(0.516)	(0.359)	(0.294)	(0.269)	(0.275)	(0.287)	(0.390)	(0.500)
Fire	-0.539	-0.547	-0.668**	-1.080	-0.941*	-0.654**	-0.557*	-0.565**	-0.686**	-0.815***	-0.397	0.200
	(0.361)	(0.451)	(0.303)	(0.960)	(0.541)	(0.331)	(0.297)	(0.271)	(0.274)	(0.281)	(0.372)	(0.542)
Hail	-0.554	-0.563	-0.794***	-1.649	-0.762	-0.654*	-0.489	-0.617**	-0.704***	-0.809***	-0.385	0.195
	(0.362)	(0.473)	(0.301)	(1.456)	(0.560)	(0.349)	(0.305)	(0.278)	(0.269)	(0.276)	(0.375)	(0.513)
Multi-component model												
	-0.535	-0.546	-0.595**	-0.970	-0.411	-0.618**	-0.666**	-0.574**	-0.762***	-0.354	-0.456	0.637
	(0.359)	(0.437)	(0.298)	(0.999)	(0.429)	(0.309)	(0.278)	(0.276)	(0.275)	(0.316)	(0.344)	(0.546)

This table reports the regression coefficients of the variable GPR when regressing real GDP per capita growth on the E3CI index and its subcomponents. Single-component models report the regression coefficients obtained from regressing real GDP per capita growth on the E3CI index and its subcomponents, separately (one at a time). Multi-component model reports the regression coefficients obtained from a multivariate regression of real GDP per capita growth on the E3CI index subcomponents. These regressions contain a linear time trend and the additional control variables NCISS and GEPU. The first column reports OLS coefficients with country fixed effects. The second column reports OLS coefficients with country fixed effects and time random effects. Period weights (PCSE) standard errors are shown in parentheses in both columns. The third column reports OLS coefficients using Autometrics panel regressions. Heteroskedasticity-consistent (HCSE) standard errors are shown in parentheses. Columns (1)-(9) refer to quantile regression of the related decile, e.g., (5) refers to 0.5 quantile/median regression. *, **, and *** denote statistical significance at the 10%, 5%, and 1% level, respectively.

Table 7: NCISS coefficients, linear trend specification

	Least Squares	Least Squares w/ time effects	Least Squares Autometrics	(1)	(2)	(3)	(4)	(5)	(6)	(7)	(8)	(9)
Single-component model with												
E3CI	0.310	0.336	-0.555	-0.509	0.699	0.713	0.501	0.182	-0.021	-0.514	-1.663**	-2.766**
	(0.782)	(0.975)	(0.639)	(1.080)	(1.294)	(0.762)	(0.648)	(0.604)	(0.609)	(0.627)	(0.661)	(1.249)
Max temp	0.440	0.459	-0.505	1.029	0.910	0.885	0.623	0.194	-0.072	-0.451	-1.687**	-2.898**
	(0.787)	(0.977)	(0.640)	(1.535)	(1.137)	(0.775)	(0.648)	(0.604)	(0.605)	(0.623)	(0.662)	(1.243)
Min temp	0.301	0.324	-0.772	1.319	1.116	0.240	0.179	0.178	-0.175	-0.993*	-1.586**	-2.089*
	(0.788)	(1.014)	(0.635)	(1.984)	(1.014)	(0.755)	(0.711)	(0.683)	(0.622)	(0.600)	(0.667)	(1.143)
Drought	0.203	0.238	-0.562	0.770	0.609	0.483	0.248	0.020	-0.213	-0.607	-1.277*	-2.057*
	(0.789)	(1.001)	(0.633)	(1.569)	(1.053)	(0.812)	(0.712)	(0.667)	(0.617)	(0.610)	(0.765)	(1.087)
Wind	0.323	0.353	-0.597	0.704	0.959	0.420	0.492	0.082	0.082	-0.646	-1.762***	-2.404*
	(0.786)	(1.026)	(0.637)	(1.494)	(1.073)	(0.798)	(0.641)	(0.610)	(0.629)	(0.654)	(0.658)	(1.254)
Precipitation	0.464	0.482	-0.523	1.021	0.932	0.418	0.360	0.377	-0.129	-0.671	-1.502**	-2.456*
	(0.788)	(0.970)	(0.635)	(1.763)	(1.052)	(0.751)	(0.667)	(0.606)	(0.592)	(0.616)	(0.731)	(1.394)
Fire	0.273	0.301	-0.631	0.214	1.128	0.699	-0.021	-0.028	-0.234	-0.614	-1.455**	-2.792**
	(0.783)	(0.968)	(0.632)	(1.174)	(1.046)	(0.766)	(0.688)	(0.620)	(0.632)	(0.613)	(0.679)	(1.227)
Hail	0.344	0.372	-0.733	0.976	0.986	0.512	0.452	0.287	-0.083	-0.522	-1.452**	-2.867**
	(0.785)	(1.012)	(0.632)	(1.536)	(1.063)	(0.728)	(0.679)	(0.677)	(0.628)	(0.610)	(0.669)	(1.265)
Multi-component model												
	0.176	0.197	-0.455	0.782	0.801	0.528	0.183	0.065	-0.197	-0.763	-1.376	-0.849
	(0.803)	(0.961)	(0.649)	(1.296)	(0.968)	(0.783)	(0.715)	(0.631)	(0.599)	(0.608)	(0.900)	(1.002)

This table reports the regression coefficients of the variable NCISS when regressing real GDP per capita growth on the E3CI index and its subcomponents. Single-component models report the regression coefficients obtained from regressing real GDP per capita growth on the E3CI index and its subcomponents, separately (one at a time). Multi-component model reports the regression coefficients obtained from a multivariate regression of real GDP per capita growth on the E3CI index subcomponents. These regressions contain a linear time trend and the additional control variables GPR and GEPU. The first column reports OLS coefficients with country fixed effects. The second column reports OLS coefficients with country fixed effects and time random effects. Period weights (PCSE) standard errors are shown in parentheses in both columns. The third column reports OLS coefficients using Autometrics panel regressions. Heteroskedasticity-consistent (HCSE) standard errors are shown in parentheses. Columns (1)-(9) refer to quantile regression of the related decile, e.g., (5) refers to 0.5 quantile/median regression. *, **, and *** denote statistical significance at the 10%, 5%, and 1% level, respectively.

Table 8: GEPU coefficients, linear trend specification

	Least Squares	Least Squares w/ time effects	Least Squares Autometrics	(1)	(2)	(3)	(4)	(5)	(6)	(7)	(8)	(9)
Single-component model with												
E3CI	-0.763**	-0.781*	-0.304	-1.359**	-0.585	-0.411	-0.391	-0.300	-0.364	-0.684**	-0.405	-0.206
	(0.347)	(0.432)	(0.278)	(0.582)	(0.651)	(0.303)	(0.293)	(0.309)	(0.323)	(0.309)	(0.287)	(0.639)
Max temp	-0.845**	-0.857**	-0.398	-1.471**	-0.755	-0.479	-0.548*	-0.306	-0.400	-0.715**	-0.434	0.017
	(0.351)	(0.436)	(0.283)	(0.703)	(0.545)	(0.313)	(0.294)	(0.309)	(0.319)	(0.313)	(0.286)	(0.645)
Min temp	-0.732**	-0.745	-0.281	-1.147	-0.793*	-0.222	-0.439	-0.342	-0.198	-0.403	-0.322	-0.093
	(0.357)	(0.459)	(0.286)	(0.765)	(0.468)	(0.306)	(0.295)	(0.346)	(0.334)	(0.319)	(0.301)	(0.553)
Drought	-0.713**	-0.735	-0.346	-0.730	-0.382	-0.362	-0.411	-0.256	-0.366	-0.522*	-0.485*	-0.692
	(0.356)	(0.451)	(0.284)	(1.082)	(0.445)	(0.328)	(0.301)	(0.340)	(0.317)	(0.301)	(0.293)	(0.442)
Wind	-0.781**	-0.802*	-0.322	-0.972	-0.939*	-0.451	-0.391	-0.319	-0.342	-0.603*	-0.412	-0.131
	(0.349)	(0.455)	(0.279)	(0.661)	(0.507)	(0.307)	(0.284)	(0.321)	(0.338)	(0.319)	(0.275)	(0.628)
Precipitation	-0.863**	-0.873**	-0.454	-1.187	-0.752	-0.325	-0.504*	-0.466	-0.425	-0.547*	-0.644**	-0.406
	(0.355)	(0.436)	(0.285)	(0.840)	(0.501)	(0.318)	(0.298)	(0.313)	(0.318)	(0.301)	(0.286)	(0.679)
Fire	-0.736**	-0.754*	-0.308	-0.918	-0.434	-0.386	-0.273	-0.229	-0.373	-0.542*	-0.302	-0.218
	(0.350)	(0.432)	(0.280)	(0.571)	(0.396)	(0.323)	(0.294)	(0.306)	(0.325)	(0.309)	(0.282)	(0.627)
Hail	-0.770**	-0.789*	-0.316	-1.256*	-0.717	-0.315	-0.439	-0.392	-0.340	-0.540*	-0.349	0.043
	(0.354)	(0.456)	(0.283)	(0.711)	(0.492)	(0.314)	(0.292)	(0.335)	(0.322)	(0.310)	(0.301)	(0.635)
Multi-component model												
	-0.691*	-0.702*	-0.447	-0.759	-0.408	-0.299	-0.317	-0.304	-0.194	-0.292	-0.468	-0.743*
	(0.355)	(0.424)	(0.301)	(0.560)	(0.441)	(0.300)	(0.316)	(0.328)	(0.338)	(0.322)	(0.291)	(0.428)

This table reports the regression coefficients of the variable GEPU when regressing real GDP per capita growth on the E3CI index and its subcomponents. Single-component models report the regression coefficients obtained from regressing real GDP per capita growth on the E3CI index and its subcomponents, separately (one at a time). Multi-component model reports the regression coefficients obtained from a multivariate regression of real GDP per capita growth on the E3CI index subcomponents. These regressions contain a linear time trend and the additional control variables NCISS and GPR. The first column reports OLS coefficients with country fixed effects. The second column reports OLS coefficients with country fixed effects and time random effects. Period weights (PCSE) standard errors are shown in parentheses in both columns. The third column reports OLS coefficients using Autometrics panel regressions. Heteroskedasticity-consistent (HCSE) standard errors are shown in parentheses. Columns (1)-(9) refer to quantile regression of the related decile, e.g., (5) refers to 0.5 quantile/median regression. *, **, and *** denote statistical significance at the 10%, 5%, and 1% level, respectively.

Appendix

Table A1: Economic impact of extreme weather events, quadratic trend specification

	Least Squares	Least Squares w/ time effects	Least Squares Autometrics	(1)	(2)	(3)	(4)	(5)	(6)	(7)	(8)	(9)
Single-component models												
E3CI	-2.656***	-2.559***	-2.260***	-9.000***	-5.543***	-4.393***	-2.851***	-2.347***	-1.789**	-1.034	-0.283	0.893
	(0.738)	(0.738)	(0.713)	(1.742)	(1.193)	(1.109)	(0.801)	(0.661)	(0.705)	(0.705)	(0.776)	(0.891)
Max temp	-0.465**	-0.436**	-0.455***	-1.178**	-0.572**	-0.634***	-0.502***	-0.634***	-0.446**	-0.362*	-0.189	0.170
	(0.198)	(0.198)	(0.176)	(0.458)	(0.272)	(0.211)	(0.166)	(0.159)	(0.182)	(0.186)	(0.230)	(0.266)
Min temp	-0.912	-1.034	-0.715	1.801	0.579	-0.483	-0.014	-0.281	-1.317**	-1.127*	-1.293*	-3.065***
	(0.800)	(0.802)	(0.593)	(2.652)	(0.922)	(0.708)	(0.632)	(0.597)	(0.570)	(0.631)	(0.772)	(0.899)
Drought	-0.824	-0.766	0.221	-4.346***	-3.218***	-1.423*	-0.050	-0.123	1.137*	1.107*	1.932***	2.428***
	(0.556)	(0.555)	(0.551)	(1.056)	(0.636)	(0.766)	(0.589)	(0.639)	(0.594)	(0.574)	(0.695)	(0.863)
Wind	-3.391***	-3.409***	-2.874***	-7.581**	-4.555**	-4.356***	-3.138***	-3.480***	-2.310**	-2.782**	-2.254*	-0.658
	(1.203)	(1.202)	(1.084)	(3.470)	(2.032)	(1.404)	(0.957)	(0.879)	(1.018)	(1.120)	(1.206)	(1.722)
Precipitation	-2.724*	-2.554*	-3.843***	-0.790	-1.421	-2.400*	-3.642***	-4.296***	-4.427***	-3.866***	-4.788***	-3.412
	(1.396)	(1.390)	(1.114)	(4.611)	(1.709)	(1.226)	(1.083)	(1.036)	(1.059)	(1.115)	(1.390)	(2.627)
Fire	-1.211***	-1.158***	-0.705*	-5.255***	-3.300***	-2.303***	-1.189***	-0.979**	-0.298	-0.069	0.556	0.907**
	(0.408)	(0.407)	(0.410)	(0.781)	(0.586)	(0.675)	(0.456)	(0.395)	(0.449)	(0.415)	(0.412)	(0.436)
Hail	0.461	0.419	0.201	1.717	0.492	0.620	0.846	1.159**	0.667	0.199	-0.034	-0.485
	(0.602)	(0.602)	(0.546)	(1.176)	(0.687)	(0.684)	(0.597)	(0.586)	(0.606)	(0.563)	(0.702)	(0.863)
Multi-component model												
Max temp	-0.599	-0.575	-0.857*	1.455	0.253	-0.473	-0.927**	-1.087**	-1.139**	-0.995*	-0.874	-0.478
	(0.573)	(0.572)	(0.468)	(0.952)	(0.546)	(0.523)	(0.449)	(0.439)	(0.460)	(0.512)	(0.732)	(0.915)
Min temp	-3.961***	-4.023***	-3.709***	0.187	-2.107*	-3.099***	-3.173***	-2.971***	-3.750***	-4.272***	-4.074***	-5.577***
	(1.126)	(1.130)	(0.924)	(2.251)	(1.187)	(0.982)	(0.934)	(0.956)	(1.016)	(1.109)	(1.515)	(1.729)
Drought	-0.955	-0.879	-0.769	-2.763*	-2.685**	-2.189**	-0.843	-0.946	-0.179	-0.075	-0.169	1.344
	(0.878)	(0.876)	(0.808)	(1.668)	(1.246)	(1.058)	(0.872)	(0.789)	(0.771)	(0.739)	(1.020)	(1.524)
Wind	-1.601	-1.900	-0.799	-0.964	-2.271	-1.983	-0.289	0.199	0.757	-1.025	-3.909*	-6.086*
	(1.833)	(1.830)	(1.420)	(3.198)	(2.429)	(1.753)	(1.419)	(1.323)	(1.321)	(1.512)	(2.155)	(3.592)
Precipitation	-3.003	-2.781	-3.697*	-9.353**	-6.935*	-3.680	-2.755	-3.480	-2.798	-2.813	-3.389	-5.069*
	(2.608)	(2.604)	(2.144)	(4.280)	(3.577)	(2.749)	(2.206)	(2.137)	(1.990)	(2.034)	(2.427)	(2.986)
Fire	-0.743	-0.744	-0.106	-6.186***	-2.504***	-0.801	-0.064	0.642	0.693	0.772	1.708*	1.430
	(0.766)	(0.763)	(0.685)	(1.446)	(0.925)	(0.898)	(0.672)	(0.661)	(0.651)	(0.667)	(0.947)	(1.302)
Hail	-2.152***	-2.166***	-1.980***	-1.719	-2.047**	-1.181	-1.141	-1.041	-1.342*	-1.797**	-1.519	-1.118
	(0.832)	(0.834)	(0.664)	(1.429)	(0.974)	(0.817)	(0.712)	(0.733)	(0.747)	(0.773)	(1.082)	(1.594)

This table reports the regression coefficients obtained from regressing real GDP per capita growth on the E3CI index and its subcomponents. Single-component models report the regression coefficients obtained from regressing real GDP per capita growth on the E3CI index and its subcomponents, separately (one at a time). Multi-component model reports the regression coefficients obtained from a multivariate regression of real GDP per capita growth on the E3CI index subcomponents. These regressions contain a quadratic time trend and the additional control variables NCISS, GPR, and GEPU. The first column reports OLS coefficients with country fixed effects. The second column reports OLS coefficients with country fixed effects and time random effects. Period weights (PCSE) standard errors are shown in parentheses in both columns. The third column reports OLS coefficients using Autometrics panel regressions. Heteroskedasticity-consistent (HCSE) standard errors are shown in parentheses. Columns (1)-(9) refer to quantile regression of the related decile, e.g., (5) refers to 0.5 quantile/median regression. *, **, and *** denote statistical significance at the 10%, 5%, and 1% level, respectively.

Table A2: GPR coefficients, quadratic trend specification

	Least Squares	Least Squares w/ time effects	Least Squares Autometrics	(1)	(2)	(3)	(4)	(5)	(6)	(7)	(8)	(9)
Single-component model with												
E3CI	-0.546	-0.555	-0.630**	-1.538*	-0.603	-0.701**	-0.635**	-0.543*	-0.526*	-0.730**	-0.406	0.157
	(0.362)	(0.462)	(0.309)	(0.912)	(0.423)	(0.315)	(0.289)	(0.279)	(0.284)	(0.296)	(0.430)	(0.515)
Max temp	-0.541	-0.550	-0.656**	-1.756	-0.539	-0.591*	-0.508*	-0.598**	-0.491*	-0.741**	-0.310	0.145
	(0.362)	(0.459)	(0.306)	(1.234)	(0.465)	(0.330)	(0.289)	(0.279)	(0.277)	(0.292)	(0.452)	(0.517)
Min temp	-0.562	-0.574	-0.795***	-1.535	-0.685	-0.619*	-0.443	-0.519*	-0.752***	-0.884***	-0.547	0.604
	(0.364)	(0.481)	(0.304)	(2.099)	(0.451)	(0.346)	(0.299)	(0.267)	(0.266)	(0.267)	(0.391)	(0.536)
Drought	-0.540	-0.550	-0.702**	-1.472	-0.510	-0.453	-0.451	-0.625**	-0.737***	-0.857***	-0.379	0.397
	(0.364)	(0.474)	(0.310)	(1.254)	(0.408)	(0.341)	(0.300)	(0.271)	(0.264)	(0.284)	(0.404)	(0.506)
Wind	-0.550	-0.561	-0.680**	-1.219	-0.753*	-0.498	-0.668**	-0.552*	-0.615**	-0.596*	-0.303	0.172
	(0.362)	(0.486)	(0.304)	(1.236)	(0.434)	(0.342)	(0.289)	(0.283)	(0.281)	(0.317)	(0.435)	(0.505)
Precipitation	-0.554	-0.563	-0.725**	-1.788	-0.582	-0.788**	-0.498*	-0.644**	-0.550**	-0.721**	-0.356	0.236
	(0.362)	(0.457)	(0.307)	(1.903)	(0.438)	(0.356)	(0.290)	(0.272)	(0.278)	(0.304)	(0.444)	(0.522)
Fire	-0.532	-0.541	-0.657**	-1.156	-0.467	-0.659**	-0.628**	-0.544**	-0.696**	-0.884***	-0.397	0.249
	(0.362)	(0.456)	(0.307)	(0.984)	(0.391)	(0.331)	(0.291)	(0.273)	(0.275)	(0.273)	(0.419)	(0.546)
Hail	-0.554	-0.565	-0.789***	-1.893	-0.486	-0.631*	-0.459	-0.553**	-0.694**	-0.846***	-0.368	0.177
	(0.364)	(0.482)	(0.304)	(1.652)	(0.426)	(0.349)	(0.299)	(0.277)	(0.270)	(0.271)	(0.435)	(0.532)
Multi-component model												
	-0.531	-0.543	-0.577*	-0.954	-0.483	-0.610**	-0.682**	-0.622**	-0.773***	-0.388	-0.529	0.597
	(0.361)	(0.432)	(0.301)	(1.059)	(0.386)	(0.308)	(0.273)	(0.282)	(0.274)	(0.346)	(0.359)	(0.570)

This table reports the regression coefficients of the variable GPR when regressing real GDP per capita growth on the E3CI index and its subcomponents. Single-component models report the regression coefficients obtained from regressing real GDP per capita growth on the E3CI index and its subcomponents, separately (one at a time). Multi-component model reports the regression coefficients obtained from a multivariate regression of real GDP per capita growth on the E3CI index subcomponents. These regressions contain a quadratic time trend and the additional control variables NCISS and GEPU. The first column reports OLS coefficients with country fixed effects. The second column reports OLS coefficients with country fixed effects and time random effects. Period weights (PCSE) standard errors are shown in parentheses in both columns. The third column reports OLS coefficients using Autometrics panel regressions. Heteroskedasticity-consistent (HCSE) standard errors are shown in parentheses. Columns (1)-(9) refer to quantile regression of the related decile, e.g., (5) refers to 0.5 quantile/median regression. *, **, and *** denote statistical significance at the 10%, 5%, and 1% level, respectively.

Table A3: NCISS coefficients, quadratic trend specification

	Least Squares	Least Squares w/ time effects	Least Squares Autometrics	(1)	(2)	(3)	(4)	(5)	(6)	(7)	(8)	(9)
Single-component model with												
E3CI	0.235	0.272	-0.733	-0.520	-0.294	0.325	0.122	0.118	-0.183	-0.390	-1.644**	-3.267**
	(0.901)	(1.134)	(0.720)	(1.630)	(1.342)	(0.833)	(0.783)	(0.745)	(0.729)	(0.691)	(0.696)	(1.286)
Max temp	0.371	0.400	-0.642	1.279	0.301	0.403	0.284	-0.117	-0.180	-0.374	-1.603**	-3.340**
	(0.907)	(1.133)	(0.711)	(1.798)	(1.256)	(0.873)	(0.768)	(0.732)	(0.726)	(0.687)	(0.699)	(1.282)
Min temp	0.328	0.365	-0.807	1.719	0.316	-0.095	0.009	0.042	-0.225	-0.747	-1.607**	-2.311**
	(0.911)	(1.186)	(0.711)	(2.099)	(1.168)	(0.883)	(0.827)	(0.799)	(0.731)	(0.679)	(0.697)	(1.156)
Drought	0.165	0.209	-0.630	1.388	-0.133	0.243	-0.024	-0.212	-0.129	-0.571	-0.994	-2.496**
	(0.914)	(1.170)	(0.708)	(1.870)	(1.214)	(0.927)	(0.827)	(0.794)	(0.714)	(0.679)	(0.814)	(1.246)
Wind	0.322	0.359	-0.571	1.167	0.222	0.302	0.102	-0.139	0.084	-0.642	-1.739**	-3.387**
	(0.907)	(1.196)	(0.720)	(1.664)	(1.219)	(0.892)	(0.780)	(0.760)	(0.740)	(0.712)	(0.692)	(1.246)
Precipitation	0.478	0.502	-0.598	2.058	0.281	0.327	0.085	0.233	-0.128	-0.636	-1.290	-2.428
	(0.912)	(1.133)	(0.707)	(1.974)	(1.215)	(0.859)	(0.796)	(0.745)	(0.693)	(0.669)	(0.785)	(1.535)
Fire	0.196	0.233	-0.750	-0.037	-0.492	0.097	-0.495	-0.366	-0.273	-0.450	-1.367*	-3.501***
	(0.903)	(1.123)	(0.705)	(1.463)	(1.168)	(0.889)	(0.819)	(0.745)	(0.741)	(0.680)	(0.705)	(1.190)
Hail	0.348	0.383	-0.791	1.491	0.020	0.279	-0.128	-0.028	-0.077	-0.403	-1.499**	-3.351**
	(0.909)	(1.185)	(0.709)	(1.727)	(1.205)	(0.867)	(0.809)	(0.795)	(0.739)	(0.679)	(0.711)	(1.304)
Multi-component model												
	0.132	0.164	-0.650	0.733	0.317	0.125	-0.069	-0.208	-0.084	-0.530	-1.125	-0.687
	(0.918)	(1.085)	(0.726)	(1.358)	(1.043)	(0.851)	(0.813)	(0.801)	(0.703)	(0.681)	(0.925)	(1.257)

This table reports the regression coefficients of the variable NCISS when regressing real GDP per capita growth on the E3CI index and its subcomponents. Single-component models report the regression coefficients obtained from regressing real GDP per capita growth on the E3CI index and its subcomponents, separately (one at a time). Multi-component model reports the regression coefficients obtained from a multivariate regression of real GDP per capita growth on the E3CI index subcomponents. These regressions contain a quadratic time trend and the additional control variables GPR and GEPU. The first column reports OLS coefficients with country fixed effects. The second column reports OLS coefficients with country fixed effects and time random effects. Period weights (PCSE) standard errors are shown in parentheses in both columns. The third column reports OLS coefficients using Autometrics panel regressions. Heteroskedasticity-consistent (HCSE) standard errors are shown in parentheses. Columns (1)-(9) refer to quantile regression of the related decile, e.g., (5) refers to 0.5 quantile/median regression. *, **, and *** denote statistical significance at the 10%, 5%, and 1% level, respectively.

Table A4: GEPU coefficients, quadratic trend specification

	Least Squares	Least Squares w/ time effects	Least Squares Autometrics	(1)	(2)	(3)	(4)	(5)	(6)	(7)	(8)	(9)
Single-component model with												
E3CI	-0.709	-0.732	-0.174	-1.148	0.126	-0.233	-0.123	-0.257	-0.291	-0.752**	-0.417	0.361
	(0.464)	(0.589)	(0.369)	(1.197)	(0.608)	(0.373)	(0.391)	(0.413)	(0.401)	(0.365)	(0.374)	(0.846)
Max temp	-0.794*	-0.813	-0.298	-1.657	-0.263	-0.211	-0.377	-0.141	-0.320	-0.767**	-0.509	0.255
	(0.468)	(0.591)	(0.366)	(1.081)	(0.773)	(0.403)	(0.376)	(0.401)	(0.403)	(0.368)	(0.364)	(0.868)
Min temp	-0.752	-0.775	-0.256	-1.539	-0.249	-0.003	-0.166	-0.230	-0.195	-0.610	-0.318	-0.036
	(0.476)	(0.627)	(0.371)	(1.110)	(0.688)	(0.421)	(0.383)	(0.431)	(0.405)	(0.387)	(0.399)	(0.696)
Drought	-0.685	-0.713	-0.296	-1.076	0.132	-0.143	-0.152	-0.176	-0.415	-0.523	-0.615*	-0.012
	(0.475)	(0.615)	(0.371)	(1.461)	(0.624)	(0.430)	(0.388)	(0.428)	(0.400)	(0.370)	(0.368)	(0.694)
Wind	-0.781*	-0.806	-0.341	-1.201	-0.330	-0.217	-0.160	-0.246	-0.340	-0.652*	-0.424	0.310
	(0.467)	(0.623)	(0.367)	(0.987)	(0.749)	(0.406)	(0.381)	(0.418)	(0.417)	(0.378)	(0.357)	(0.849)
Precipitation	-0.873*	-0.888	-0.399	-1.688	-0.244	-0.125	-0.238	-0.357	-0.423	-0.583	-0.828**	-0.217
	(0.476)	(0.597)	(0.369)	(1.326)	(0.720)	(0.420)	(0.387)	(0.410)	(0.403)	(0.359)	(0.358)	(0.923)
Fire	-0.679	-0.703	-0.221	-0.602	0.331	-0.034	0.074	-0.042	-0.344	-0.642*	-0.389	0.413
	(0.468)	(0.587)	(0.365)	(1.061)	(0.487)	(0.416)	(0.389)	(0.396)	(0.400)	(0.374)	(0.366)	(0.737)
Hail	-0.773	-0.797	-0.274	-1.842*	-0.085	-0.243	-0.121	-0.117	-0.316	-0.641*	-0.332	0.263
	(0.474)	(0.625)	(0.369)	(1.049)	(0.714)	(0.418)	(0.388)	(0.423)	(0.400)	(0.370)	(0.379)	(0.873)
Multi-component model												
	-0.659	-0.677	-0.304	-0.662	0.201	0.049	-0.167	-0.126	-0.310	-0.447	-0.530	-0.797
	(0.471)	(0.560)	(0.390)	(0.828)	(0.536)	(0.378)	(0.413)	(0.437)	(0.420)	(0.380)	(0.370)	(0.591)

This table reports the regression coefficients of the variable GEPU when regressing real GDP per capita growth on the E3CI index and its subcomponents. Single-component models report the regression coefficients obtained from regressing real GDP per capita growth on the E3CI index and its subcomponents, separately (one at a time). Multi-component model reports the regression coefficients obtained from a multivariate regression of real GDP per capita growth on the E3CI index subcomponents. These regressions contain a quadratic time trend and the additional control variables NCISS and GPR. The first column reports OLS coefficients with country fixed effects. The second column reports OLS coefficients with country fixed effects and time random effects. Period weights (PCSE) standard errors are shown in parentheses in both columns. The third column reports OLS coefficients using Autometrics panel regressions. Heteroskedasticity-consistent (HCSE) standard errors are shown in parentheses. Columns (1)-(9) refer to quantile regression of the related decile, e.g., (5) refers to 0.5 quantile/median regression. *, **, and *** denote statistical significance at the 10%, 5%, and 1% level, respectively.